SYNTHESIS OF Ni AND Zn BASED ORGANIC FRAMEWORKS AS PHOTOCATALYST

A Thesis Submitted to
the Graduate School of Engineering and Sciences of
İzmir Institute of Technology
in Partial Fulfillments of the Requirements for the Degree of

MASTER OF SCIENCE

in Chemical Engineering

by
Merve DİKMEN

July 2019
İZMİR

We approve the thesis of **Merve DİKMEN**

Examining Committee Members:

_____
Prof. Dr. Fehime ÇAKICIOĞLU ÖZKAN
Department of Chemical Engineering, İzmir Institute of Technology

_____
Assist. Prof. Dr. Ayben TOP
Department of Chemical Engineering, İzmir Institute of Technology

_____
Assoc. Prof. Dr. Meral DÜKKANCI
Department of Chemical Engineering, Ege University

18 July 2019

_____
Prof. Dr. Fehime ÇAKICIOĞLU ÖZKAN
Supervisor, Department of Chemical Engineering
İzmir Institute of Technology

_____
Prof. Dr. Erol ŞEKER
Head of Department of Chemical Engineering

_____
Prof. Dr. Aysun SOFUOĞLU
Dean of Graduate School of Engineering and Sciences

ACKNOWLEDGMENTS

I would like to offer my deepest appreciation and warmest gratitude to my advisor, Prof. Dr. Fehime ÇAKICIOĞLU ÖZKAN for her supervision, support, encouragement and patience in my thesis study.

I would like to thank Prof. Dr. Şerife Şeref HELVACI for UV-Vis analysis.

I am thankful to technical staff who carried out the ATR-IR, XRD and SEM analysis.

I would like to thank the technical staff of Department of Chemical Engineering for their technical assistance and help during the laboratory works.

I would like to thank my dear friend Ceren ORAK because she always supported and encouraged me during my whole study. I am thankful to my beloved romie Canan TAŞ for her endless support, tolerance and understanding in my whole university life.

Finally, I must express my deepest thanks to my family; my mother Nazife DİKMEN, my father Hüseyin DİKMEN and my brother Faruk DİKMEN. I am really grateful for providing me with unfailing support, continious encouragement and motivation throughout my years of study. I knew that they were always there for me, whenever I needed them. If they were not my family, i could not success my study.

ABSTRACT

SYNTHESIS OF Ni AND Zn BASED ORGANIC FRAMEWORKS AS PHOTOCATALYST

Nickel (Ni) and zinc (Zn) based organic frameworks were synthesized on the synthetic zeolite (5A and 13X), natural zeolite mineral clinoptilolite, α-Alumina. Initially the zeolite surface was modified or seeded with metal organic framework (MOF). MOF-zeolite composite materials were characterized with XRD, SEM and ATR-IR to understand whether surface processes was achieved successfully or not. Additionally, band gap energies were evaluated to understand these composite materials were used as photocatalyst. Surface modification with APTES was not affect surface of the zeolites. In spite of that seeding created a layer on the surface of zeolite. Nickel based organic framework was coated onto the surface of modified 5A surface. Hydrothermal ZIF8 (ZIF8(1)) and solvothermal ZIF8 (ZIF8(2)) were synthesized successfully as MOF crystals. Besides ZIF8(2) was coated onto the surface of natural zeolite. Additionally, ZIF8/CuBTC sample were synthesized, seeded and coated onto the surface of natural zeolite. Band gap energies of the MOFs and composite materials were calculated with Tauc plot. Results showed that UV light can be used as light source for photocatalytic reactions of these photocatalysts. Also increasing photocatalyst amount increased dye degredation under UV light.

ÖZET

FOTOKATALİZÖR OLARAK Ni VE Zn TEMELLİ ORGANİK AĞ YAPILARININ SENTEZİ

Nikel ve çinko temelli organic ağ yapıları, zeolit 5A ve 13X, doğal zeolite ve alüminyum oksit'in yüzey işlemleri ve doğrudan sentez ve kaplama metotları ile yapılan metal organik ağ yapıları ile zeolitlerin oluşturduğu birleşik maddeler araştırılmıştır. Bu maddeler yüzey işlemlerinin başarılı olup olmadığını anlayabilmek için XRD, SEM ve ATR-IR ile analiz edilmiştir. Ayrıca bu birleşik maddelerin fotokatalizör olarak kullanılabileceği bant aralığı enerjileri incelenerek anlaşılmıştır. Yüzey modifikasyon işlemlerinden APTES isimli kimyasal ile yapılanın zeolite yüzeyine bir etkisi görülmemiştir. Buna karşın MOF kaplama işlemini kolaylaştırması için yapılan tutunma yüzeyi oluşturma işlemi başarı ile sonuçlanmıştır. Nikel temelli metal organic ağ yapısı yüzeyine modifikasyon işlemi uygulanmış zeolite 5A'nın yüzeyine başarı ile kaplanmıştır. ZIF8 isimli metal organic ağ yapısı iki farklı metot ile sentezlenmiş olup sentez sırasında çözücü olarak metil alkol kullanılan ürün ayrıca doğal zeolite üzerine de kaplanmıştır. Kaplama işlemi başarı ile gerçekleştirilmiştir. Buna ek olarak, ZIF8 ve bakır içeren metal organic ağ yapısı kompozit ürün olarak sentezlenmiş olup, bu ürün doğal zeolitin üzerine de sentezlenmiştir. Bu fotokatalizörlerin bant aralığı enerjileri incelenmiş olup UV ışık kaynağı ile fotokataliz reaksiyonlarının gerçekleştirilebileceği görülmüştür. Ayrıca yapılan UV ışığı kaynaklı deneyler sonucunda artan fotokatalizör miktarının solüsyondaki Rhodamine-B isimli boyayı bozundurduğu gözlemlenmiştir.

Dedicated to my grandmother and grandfather…

TABLE OF CONTENTS

LIST OF FIGURES

Figure **Page**

Figure **Page**

LIST OF TABLES

Table **Page**

CHAPTER 1

INTRODUCTION

Indoor air quality is gained importance due to the industrialization and urbanisation. Indoor air pollution affects human health which causes fatal diseases for instance pneumonia and cancer. Asbestos, carbon monoxide, pesticides, tobacco smoke and volatile organic compounds (VOCs) are the sources of indoor air pollution. Volatile organic compounds have toxic and carginogenic effects that cause liver, kidney and nervous system damages and cancer. Boiling point of VOCs are between 50-260 °C. This causes for evaporation of VOCs under normal conditions. Paintings, cleaning products, tobacco smoke are the basic sources of VOCs. Toluene, acetic acid, xylene, formaldehyde and diethyl ether are the VOCs examples (Yang et al., 2019).

Additionally, water consumption increases, so that the reuse of wastewater and its treatment becomes a major concern. In this respect, photocatalysis, which means adsorption of photons, is the most common process for wastewater treatment. It can be used for heavy metal and VOC elimination from wastewater and air, respectively. Various catalysts and catalyst support materials can be used in photocatalysis. Most commonly used supporting materials are zeolites, metal organic frameworks (MOFs) and their composites.

MOFs are highly porous materials composed of a metal ion and an organic ligand. They have diversity in their structure depending on the metal ion or organic ligand which are used for synthesis of the metal organic framework.

Zeolites are natural or synthetic porous crystalline alumina silicates which contain AlO_4 tetrahydra and SiO_4. They have cages in their structure and can be used as adsorbent, ion exchanger and catalyst. Natural zeolites are formed from volcanic eruption residuals for instance lava or ash and minerals. Most abundant natural zeolite is clinoptilolite. They can be obtained from same source but used for different applications. They does not have stability, so that it is a disadvantage (Mgbemere et al. 2017). Additionally, if they

compose from volcanic materials they have impurities in their pores. For example metal ions were remained within the pores of zeolite (Moshoeshoe et al. 2017). Raw materials of synthetic zeolites are silicic acid and sodium aluminate for ZSM-5, rice husk and halloysite mineral for NaA zeolite, kaolin for NaX and zeolite Y and SiO_2 sinter and perlite glass for zeolite Y. Christidis et al. synthesized zeolite from silica and perlite to obtain zeolite Y (Christidis et al. 2008). Htay and Oo synthesized zeolite Y from kaolin and sodium hydroxide (Htay et al. 2008). Ma et al., produced NaX zeolite from kaolin (Ma et al. 2014). Kovo et al., synthesized a ZSM-5 zeolite from kaolin (Kovo et al. 2009).

Composite materials are synthesized with coating of MOFs onto the support surface to eliminate the disadvantages of support material and MOFs. They show the properties of supports and coated materials MOFs.

The aim of this study is that the coating or layering of support surfaces with a MOF to use them as a photocatalyst. Zeolite 5A bead, zeolite 13X powder, α-alumina and natural zeolite clinoptilolite will be chosen as support and their surfaces coated with nickel containing MOF (Ni-MOF74) and zeolitic imidazolate framework (ZIF8). In addition, copper based MOFs will be deposited onto zeolitic imidazolate framework (CuBTC@ZIF8). Then their photocatalytic activities will be analyzed.

CHAPTER 2

PHOTOCATALYSTS

The photocatalyst is a semiconductor to promote photocatalysis reactions. They are used in the conversion of solar energy into chemical energy and abatement of pollution in air and water especially for the elimination of volatile organic compounds (VOCs), CO_2 reduction and photoinduced self-cleaning. TiO_2, ZnO, Fe_2O_3, CdS, and ZnS have commonly used photocatalysts. TiO_2 is the most common photocatalyst and highly reactive, less toxic, chemically stable and inexpensive.

Fujishima and Honda examined the photocatalytic properties of TiO_2 by water splitting in a photo electrochemical cell. This application, known as the Honda-Fujishima effect was used in water treatment processes (Fujishima and Honda., 1972).

Metal organic frameworks have an opportunity to use as a photocatalyst. Since they have adjustable properties for example pore size and surface area. For instance, iron (Fe-) based metal organic frameworks (MIL-53, MIL-68, and MIL-100) have a photocatalytic property with their metal-oxo cluster in the visible light region.

The metal organic frameworks or metal oxides are deposited on the support such as zeolite, alpha alumina, silıcon oxide as photocatalyst. Both nanoparticles and MOF properties exist in new composite material. Magnetic, electrical and catalytic properties come from nanoparticle core and ordered crystalline pores, flexibility, and multi-coordination sites come from MOFs shell. They have high stability, dispersibility, and multi-functionality. These properties provide aggregation, undesirable dissolution, and corrosion (Liu et al. 2019).

Yang et al. investigated the photocatalytic activity of Zn-based organic framework and its composites. Photocatalytic degredation of rhodamine B under ultraviolet light was examined and It was observed that synthesized ZnO on MOF5(Zn-based metal organic framework) composite material had better catalytic activity by comparing the commercial TiO_2 catalyst according to adsorption capacities (Yang et al. 2011).

Mohaghegh et al. reported that the photocatalytic activity of multifunctional MIL-88B(Fe)-Ag/TiO_2 nanotubes/Ti. They synthesized MIL88B(Fe)-Ag/TiO_2 nanotubes/Ti composite to enhance the photocatalytic activity of TiO_2. Investigation of photocatalytic activity was observed with purifying of organic, inorganic and biological pollutants from water. Adsorption studies of this photocatalyst were done with Pb^{2+} and Cd^{2+} heavy metals in water. They observed that composite photocatalyst had a higher adsorption capacity than TiO_2 (Mohaghegh, Faraji, and Abedini 2018)

Photocatalysts are used as adsorbent since their porous structure. Correspondingly modified photocatalyst shows better adsorption capacity than the unmodified one. For this purpos, photocatalyts are deposited with another porous material to form a composite structure. In this study, a new composite material which was used as a photocatalyst (adsorbent) was synthesized. Therefore a MOF which has photocatalytic property was deposited onto the zeolite surface to enhance the adsorption capacity and make them more water and thermally stable.

Adsorbents are porous materials with a high surface area. They are used in adsorption processes. Removal of pollutants is performed with adsorption by using adsorbents. Additionally, adsorbents used as a catalyst. Alumina, bauxite, ion exchange resins, activated carbon, silica gel, zeolites, and metal organic frameworks are example adsorbents. Alumina is a synthetic adsorbent. It can be used in the elimination of water, decolorization, and separation of petroleum oils and waxes. Bauxite is crystalline alumina with iron oxides and kaolinite. It can be used similar applications with alumina. Additionally, it is removed aerobic and anaerobic bacteria. Another adsorbent is silica gel. It composes of silicic acid with coagulation. Silica gel is used in drying and purifying industries. Ion exchange resin is also an adsorbent. This type of adsorbents has two group cation and anion exchange resins. Cation exchange resins compose of mostly sulfonic acid groups and a small quantity of carboxylic or phosphoric groups. Anionic resins have strong and weak ammonium groups. Organic compounds elimination are achieved with ion exchange resins. The last adsorbent of this part is activated carbon. Resources of activated carbon are wood, coal, etc. Physical and chemical activation is the production methods of activated carbon. Physical activation occurs at high temperatures. In spite of this chemical, activation takes place lower temperatures than physical activation. It is used in water and wastewater treatment, metal ion adsorption from water and purification of dye and phenol (Gupta et al. 2009).

2.1. Zeolites as support

Zeolites, crystalline materials (Gupta et al. 2009) are used in the purification of drinking water, municipal and industrial wastewater, separation of hydrocarbons, gas separation, some medical applications for example cancer treatment, a chemical sensor and catalysis (Moshoeshoe et al. 2017). Natural zeolites are mostly obtained from volcanic rocks containing minerals. Clinoptilolite is a natural zeolite mineral. Synthetic zeolites are good alternatives for natural zeolites. For instance, thermal breaking or cracking is cheaper than using natural zeolite instead of its expensive alternative synthetic zeolite. Natural zeolites are low-cost but they are not pure. They may contain metals or crystals. On the other hand, synthetic zeolites are produced favorably to applications with purer than natural zeolites. This is the most important advantage for synthetic zeolites. Consequently, the adsorption capacity of synthetic zeolites higher than natural zeolites (Moshoeshoe et al. 2017).

A type zeolites are aluminasilicates and a member of molecular sieves. Three subgroups are present in this type, 3A, 4A, and 5A. Na, Ca, K are the cations which are found in the surface of the zeolite. 4A zeolite has Na+ as cation on the surface. Pore opening of this zeolite is 4.1 A. because of this, it is said molecular sieve 4A zeolite. If the K+ replaces to the Na+ which is present on the surface of 4A zeolite, new zeolite are named as molecular sieve 3A. Since K^+ ion is larger than Na^+ ion so pore opening decreases to approximately 3A. By contrast with this, when Na^+ ion exchanges with Ca^{2+} ion pore opening becomes 5A. As a result, this zeolite is labelled as molecular sieve 5A (Julbe et al. 2016).

2.1.1. Surface Modification of Supports

MOF/zeolite, polymer/zeolite, MOF/activated carbon composites are recently studied as photocatalysis to increase the adsorption and/or degradation capacity these composite adsorbents. Zeolites (natural or synthetic), activated carbon or α-alumina , polymers, etc. can be used as support materials. Pre-treatment is needed for support before synthesizing these composite adsorbents. Modification of support surface improves the interaction between the coating material and the support surface. For example, Al-Naddaf

et al. modified molecular sieve 5A surface with succinic anhydride, 3-aminopropyl triethoxysilane, and DMF to form the carboxyl group on the surface of zeolite 5A (Al-Naddaf, Thakkar, and Rezaei 2018). Another study about surface modification is the acid treatment of the support surface. Amereh et al. treated natural zeolite clinoptilolite surface with HNO_3 solution. For this purpose, 8M HNO_3 solution and clinoptilolite were mixed and heated at 80 $^{\circ}C$ for 8 h. HNO_3^- treated clinoptilolite is inexpensive support and promotes toluene oxidation (Amereh et al. 2018)

Seeding is a surface modification method which is preparing the support surface for layering with MOF.

2.2. Metal Organic Frameworks

Metal organic frameworks (MOFs) are identified as a metal cluster linked with an organic ligand. These structures are named also coordination polymers, a hybrid organic inorganic material or organic zeolite analogues with unavoidable overlap (Rowsell et al. 2004).

MOFs are microporous or mesoporous materials with high surface area, crystal structure, tunable pore size, and variable chemical functionality. They are a good candidate for gas adsorption and separation (Wu et al. 2013). Since the functionality in the pore size of MOFs makes them better adsorbent than traditional adsorbents, for example, zeolites and activated carbons (Grant Glover et al. 2011).

2.2.2. Ni-MOF74

MOF-74 is a type of MOF with metal ion Co, Mg, Fe, and Ni. MOF-74 has the open metal site, unsaturated metal center. This open metal site increases the adsorption capacity of MOF with having extra binding sites. During synthesis solvents (H_2O or DMF) expose to the pores of synthesized MOF. Despite this solvent can be removed from MOF with vacuum easily owing to open metal sites.

MOF-74 can be used in hydrogen storage, CO_2 capture and separation of CO_2-CH_4-H_2 or CO_2-CH_4 gas mixture (Wu et al. 2013).

The conventional solvothermal method is a synthesis method for MOF-74. Merely this method is a time consuming method. Synthesis time varies from 20 h to 3 days. Alternatively, ultrasound, surfactant-assisted and microwave assisted methods are used lately. Since they occur in a short time. Nevertheless adsorption capacity of alternative methods is lower than the conventional method (Wu et al. 2013).

Glover et al. examined that the separation of harmful gases from breathing air, sulfur dioxide, ammonia, octane, and gases from the industry. For this purpose, they studied with low pressure adsorption. They synthesized MOF-74 with metal ions Mg, Co, Ni, and Zn. Mg-MOF-74 had the highest surface area compared with other synthesized adsorbents. Additionally, they studied at dry and wet conditions and found that at wet conditions MOF-74 adsorbs water present at the environment. Thus adsorption capacity for gas adsorption was decreased (Grant Glover et al. 2011).

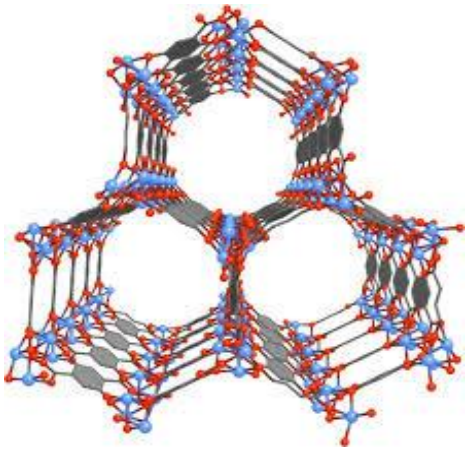

Figure 2. 1. Structure of Ni-MOF74 (Source: Grant Glover et al. 2011)

2.2.3. ZIF-8

Zeolitic imidazole frameworks (ZIFs) have a structure like zeolites. Nevertheless, they are a subgroup of MOFs. Zn (ZIF-8), Co (ZIF-67) and Cu (Cu/ZIF-8) are the metal clusters for ZIF which is linked with imidazole. The microporous structure of ZIFs depends on the ring number of the metal ions tetrahedral. According to four-, six-, eight- and twelve- membered rings pore size could be arranged. Even though ZIFs have zeolite like structure, the pore size of ZIFs are greater than the zeolites pore size. Since the tunable pore sizes of ZIFs.

In this study, zeolitic imidazolate framework-8, ZIF-8, was used which was composed of $Zn(NO_3)_2$. $6H_2O$ and 2-methyl imidazole. ZIF-8 is more thermally and chemically stable when compared to other MOFs. This stability is examined with benzene, methanol and aqueous sodium hydroxide. Besides, the crystal structure of ZIF-8 remains stable at atmospheric conditions up to 300 °C for 5 h and up to 400 °C for 5 h under argon gas flow (Jafari et al. 2018).

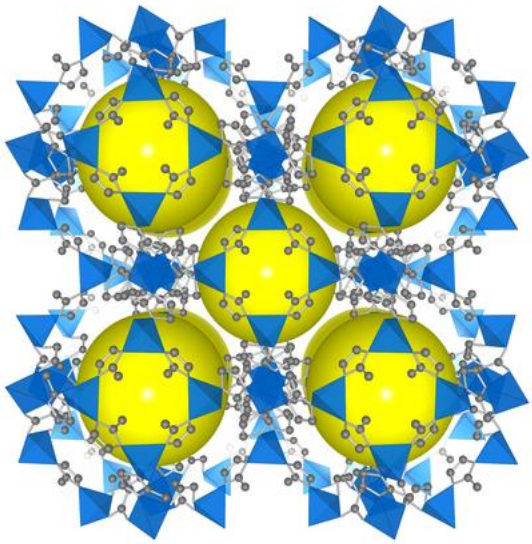

Figure 2. 2. Structure of ZIF-8 (Source: Fujie et al. 2015)

A disadvantage of MOFs is instability against water. In spite of this, ZIF-8 is water stable. Pan et al. examined the stability of ZIF-8 using boiling water for 5 days. At the end of 5 days the structure of ZIF-8 did not change with water. Likewise, they explored ZIF-8 stayed stable under atmospheric air at 200 °C for 24 h. (Pan et al. 2011) In addition to that, Zhang et al. investigated the separation of EtOH water solution. They obtained a result about hydrophobicity of ZIF-8 (Zhang, Li, and Chen 2013). Chemical stability of ZIF-8 was evaluated under high pressures (Hu et al. 2011).

ZIF-8 is synthesized by solvothermally, microwave-assisted, sonochemical, mechanochemical, microfluidic method or dry-gel conversion. Lee et al. examined all of the synthesis methods for ZIF-8 production. In solvothermal synthesis, MeOH and DMF could be used as a solvent. Synthesis temperature of this procedure was 140 °C for 24 h. In order to eliminate unreacted chemicals solid was washed with DMF and MeOH. DMF was used as a solvent and placed in a microwave oven at 120 °C and 80 W for 3 h in the microwave-assisted method. The washing step was done by using DMF and MeOH.

Another method is the mechanochemical synthesis method which was investigated by using DMF and MeOH for purification. DMF was used as solvent and oil bath at 150 °C was needed. Also, DMF and MeOH were used again for washing. For dry-gel conversion water was used as a solvent. The synthesis was done in an autoclave at 120 °C for 24 h. Product was washed with water in this method (Lee et al. 2015).

The solvent is an important parameter for ZIF-8 synthesis. Solvents used in the synthesis of ZIF-8 are mostly harmful to human health and environment. Besides, they are toxic and expensive. For this reason, alternative synthesis routes are experienced. Bao et al. used methanol as a solvent in their study (Bao et al. 2013). Smith et el. tried aliphatic alcohols as a solvent to examine the solvent effect on ZIF-8 production (Smith et al. 2009).

Jafari et al. studied with the elimination of toluene and carbon tetrachloride. For this purpose, they synthesized diluted and concentrated ZIF-8. They used a fixed bed reactor system for adsorption of toluene and carbon tetrachloride. Before adsorption ZIF-8 which was used as adsorbent thermally treated with dry air at 200 and 300 °C for 5 h. Increasing temperature from 200 °C to 300 °C increased carbon tetrachloride adsorption capacity for diluted ZIF-8 sample from 44.86 to 68.11 mg g^{-1} for concentrated ZIF-8 sample from 75.27 to 98.31 mg g^{-1}. The adsorption capacity of diluted ZIF-8 raised from 71.87 to 138.51 mg g^{-1} and adsorption capacity of concentrated ZIF-8 raised from 148.62 to 381.53 mg g^{-1} for toluene when treatment temperature increased from 200 °C to 300 °C (Jafari et al. 2018).

Bohme et al. evaluated ethane-ethylene separation by adsorption using ZIF-8 as adsorbent. The adsorption capacity of ZIF-8 was between for ethane from 1.2 to 2.5 mmol g^{-1} and for ethylene from 0.5 to 1.5 mmol g^{-1} at temperature range 283-323 K and 1 bar (Bohme et al., 2013).

2.3 Composite Materials

MOF/zeolite, polymer/zeolite, MOF/activated carbon, and MOF/silica are the example composite adsorbents. Composite materials with MOF based are enhanced the functionality of the new material. Since after synthesis new material has raw materials properties and also has new properties (Al-Naddaf, Thakkar, and Rezaei 2018). For instance, a MOF/zeolite composite has high thermal, mechanical and structural stability

which is supplied from the zeolite part of the composite. Besides the functionality and flexibility of composite material belong to MOF (Zhu et al. 2014). Moreover, it is not adequate to adsorb small molecules with MOF. Because adsorption forces are weak between pores and adsorbents. Liquid phase epitaxy, direct synthesis, in-situ crystallization, seeded growth, and electrochemical growth are the methods for coating surfaces with MOF (Lawson et al. 2017). In electrochemistry direct application of MOF is insufficient. Since electrical conductivity of MOF was indigent. In order to solve this problem, MOFs are deposited to conductive material (Xu et al. 2014). Zhang et al. examined to make composite material with copper based MOF and macroporous carbon. An electrical property of macroporous carbon makes composite material electrocatalyst (Zhang, Li, and Chen 2013).

In addition to that, Wang et al. studied with hybrid nanocomposite materials which compose of graphene oxide and copper terephthalate MOF. After that, they used the composite as a sensor for two different drugs, acetaminophen and dopamine, in serum and urine samples. As a result of this study they detected target drugs with high sensitivity and low interference (Xu et al. 2014).

Chen et al. determined a new porous composite material which consists of graphene oxide and MOF505 by a solvothermal method. They investigated the selective adsorption of CO_2/CH_4 and CO_2/N_2 mixtures MOF505/GO composite as well as MOF505. As a consequence, they found that MOF505/GO composite had higher adsorption capacity than MOF505 (Chen et al. 2017).

Yue et al. considered that ZIF-8 (zeolitic imidazolate framework) coated multi-wall carbon nanotubes to examine the electrically conductive nanocomposites for Li-sulfur battery. They used this composite to store energy. Multi-wall nanotubes with ZIF-8 had too many electrochemical properties than ZIF-8 (Yue et al. 2014).

Table 2. 1. Surface treatment and coating methods of the support surface

Support	Pretreatment of support	Metal source	Organic ligand	Coating process	Synthesis conditions	Application area	Reference
NaY zeolite	With APTES and succinic anhydride	$Zn(NO_3)_2$	H_2BDC	Solvothermal synthesis	105 °C 12 h	Catalytic hydrogenation	Lim et al., 2016
Activated carbon	-	$Cu(OAC)_2.H_2O$	H_3BTC	Solvothermal synthesis	40 °C overnight	Electrochemical cell	Fleker et al., 2016
Beta zeolite	With APTES and succinic anhydride	$ZrOCl_2.8H_2O$	H_2BDC	Solvothermal synthesis in an oil bath	423 K 24 h	Coumarin production	Rani et al., 2018
Beta zeolite	-	$Cu(NO_3)_2.3H_2O$	H_3BTC	Solvothermal synthesis	120 °C 12 h	Removal of aromatic	Liang et al., 2018
Alpha alumina	Degassed at 373 K in water	$Cu(NO_3)_2.3H_2O$	H_3BTC	Hydrothermal synthesis	383 K 18 h 393 K 12 h	Gas purification and separation	Gascon et al., 2008
Cotton swatch	With cyanuric chloride and cysteamine	$ZrCl_4$	2-aminotereph talic acid	Hydrothermal synthesis	120 °C 24 h	Chemical warfare agent neutralizer	Bunge et al., 2018

CHAPTER 3

EXPERIMENTAL STUDY

In this study, nickel (Ni-) and zinc (Zn-) based metal organic frameworks were synthesized on the support materials for photocatalytic applications. Zeolite 5A (beads), α- alumina, zeolite 13X (powder) and natural zeolite (clinoptilolite) were chosen as support materials. The surface of support material was used as unmodified , modified or seeded forms to obtain the zeolite MOF composite.

3.1. Materials

Chemicals used in this study were analytical grade and used without purification (Table 3.1).

3.2. Methods

In this study, surface of support materials were modified or seeded and then coated with Ni-, Zn- or Cu-and Zn-based organic frameworks.

Modification of the support surfaces was done by two different methods as given in section 3.2.1. After that nickel based (Ni-MOF74), zinc based (ZIF8:zeolitic imidazolate framework), and Copper based (CuBTC) and zinc based (ZIF8) organic frameworks were coated on the molecular sieve 5A (5A), α-alumina (α), moleculer sieve 13X (13X) and natural zeolite mineral (CLN). The coating methods will be explained in 3.2.2.

Table 3. 1. The chemicals used for the treatment of support surface and synthesis of composite materials

Chemical	Brand/Purity
Moleculer sieve 5A bead	Alfa Aeser
α-alumina, α- Al_2O_3	Riedel
Moleculer sieve 13X	Sigma Aldrich
Natural zeolite	Gördes
Succinic anhydride, $C_4H_4O_3$	Merck, >98.0
(3-aminopropyl)triexhoxysilane (APTES), $C_9H_{23}NO_3Si$	Sigma Aldrich, >98.0
N,N-Dimethylformamide (DMF), $HCON(CH_3)_2$	Merck
Ethanol (EtOH), C_2H_5OH	Merck
Methanol (MeOH), CH_3OH	Merck
2,5-dihydroxyterephtalic acid (DHTA)	Sigma Aldrich, >98.0
Nickel (II) nitrate hexahydrate $Ni(NO_3)_2*6H_2O$	Sigma Aldrich
1,3,5- Benzenetricarboxylic acid (Trimesic acid)	Merck, >95.0
Zinc acetate dihydrate, $(CH_3COO)_2Zn.2H_2O$	Merck
2-Methylimidazole, CH_6N_2	Alfa Aesar
Zinc oxide, ZnO	Sigma Aldrich
Copper (II) nitrate trihydrate $Cu(NO_3)_2.3H_2O$	Merck, >99.5
Zinc nitrate hexahydrate, $N_2O_6Zn.6H_2O$	Acros Organics, >98.0

3.2.1. Modification of Support Material Surface

Zeolite 5A, α- alumina, zeolite 13X, clinoptilolite were modified by using *method 1;* clinoptilolite were also modified by using *method 2.*

Method 1: APTES modification (M)

The modification method applied by Al-Naddaf et al. was used (Figure 3.1). Briefly, 7.5 g of succinic anhydride and 18 ml of APTES was dissolved in 100 ml DMF and stirred for 25 min. at room temperature. 2.5 g support was dried under vacuum at 350 $^{\circ}$C for 3 h was added to this solution and stirred for 24 h and than filtered. After that, the support was stirred with 15 ml ethanol for 30 min. This step was repeated 5 times. After that, the modified support (support(M)) was dried under vacuum at 75 $^{\circ}$C for 12 h (Al-Naddaf, Thakkar, and Rezaei 2018).

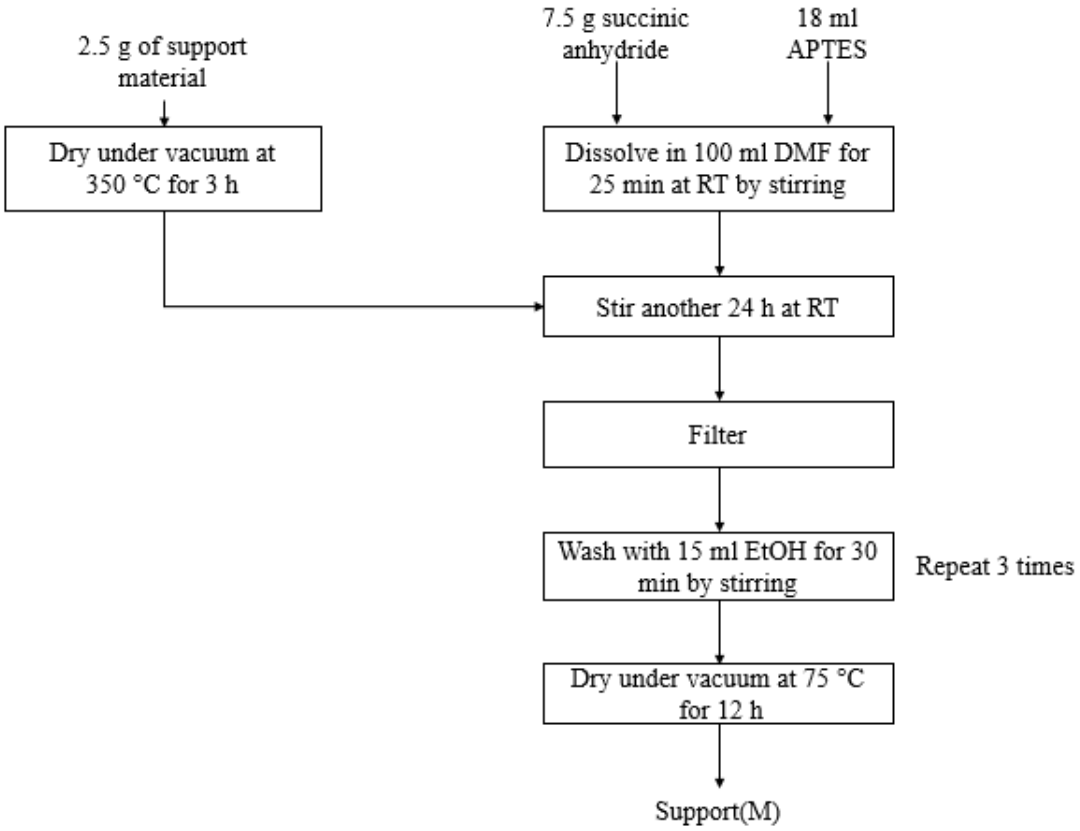

Figure 3. 1. Flow chart of surface modification method 1 (M)

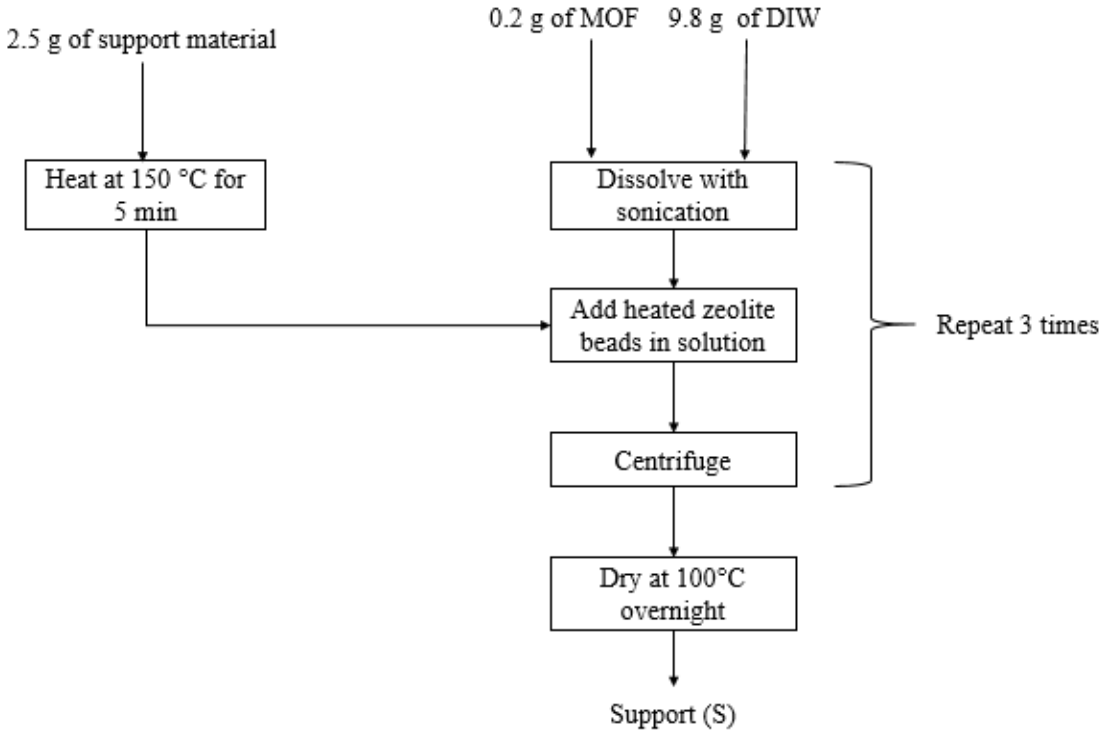

Figure 3. 2. Flow chart of surface modification method 2 (S)

Method 2: Seeding (S);

Seeding method proposed by Tate et al. was applied (Figure 3.2) for Bead Zeolite 5A, α- alumina, silicagel, zeolite 13X, natural zeolite (clinoptilolite). Briefly, 9.8 g of DI water involving 0.2 g of MOF crystals were sonicated for 10 min. Then 5 g of support materials which was heated at 150 °C for 5 min was added to the prepared solution and then centrifuged at 4500 rpm for 5 min to separate solid part. This procedure was repeated 3 times. Afterwards, support was dried at 100 °C overnight and seeded support (support(S)) were obtained (Tate et al. 2016)

3.2.2. Nickel Containing MOF-74 synthesis

Ni based MOF-74 was carried out in the two different synthesis methods.

Synthesis 1(1);

0.5 g of 2,5-dihydroxyterephtalic acid (DHTA) and 1.5 g of $Ni(NO_3)_2.6H_2O$ were sonicated in 210 ml DMF:EtOH:deionized water (DIW) (1:1:1/v:v:v) solution in a schott bottle. When the solution became clear, it was put in an oven at 100 °C for 66 h. After crystallization completed, it was cooled to the room temperature and filtered. Obtained solid was washed three times with 20 ml DMF by stirring. Then, this washing step was repeated with MeOH. Thereafter, the solid part was put in 20 ml MeOH for three days and the solvent was changed twice a day. Then they were put in an oven at 250 °C for 5 h. Lastly, Ni-MOF-74 coated zeolite 5A was separated from MeOH by filtering. In order to dry coated zeolites, they were put in an oven at 250 °C for 5 h. In order to obtain Ni-MOF-74 coated zeolite 5A, M5A was put in the sonicated solution in the procedure mentioned above (Grant Glover et al. 2011)

Synthesis 1(2);

A clear solution was prepared by dissolving 1.902 g of (6.54 mmol) $Ni(NO_3)_2.6H_2O$ and 0.382 g (1.92 mmol) (DHTA) in a solution of 159.9 ml DMF:EtOH:DIW (1:1:1 v/v/v) under sonication. The solution was placed in a Teflon lined stainless steel autoclave. The autoclave was kept at 100 °C for 24 h. Then, it was cooled to the room temperature and filtered. 20 ml MeOH was added to the solid and the solution was aged for 3 days. Finally, MOF was filtered and then washed with 20 ml MeOH by stirring and filtering after washing step and dried at room temperature. (Wu et al. 2013).

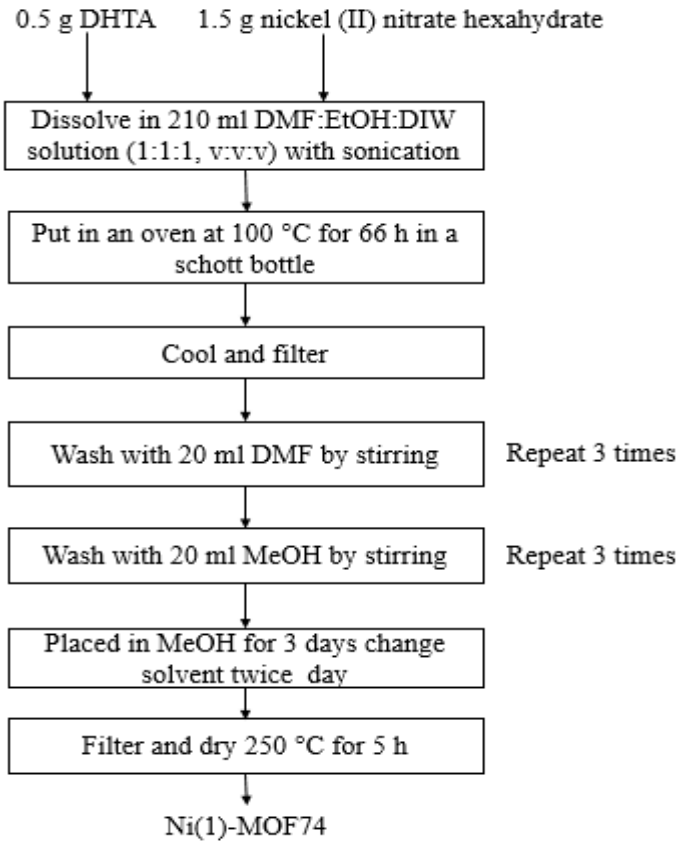

Figure 3. 3. Synthesis steps of Ni(1)-MOF74

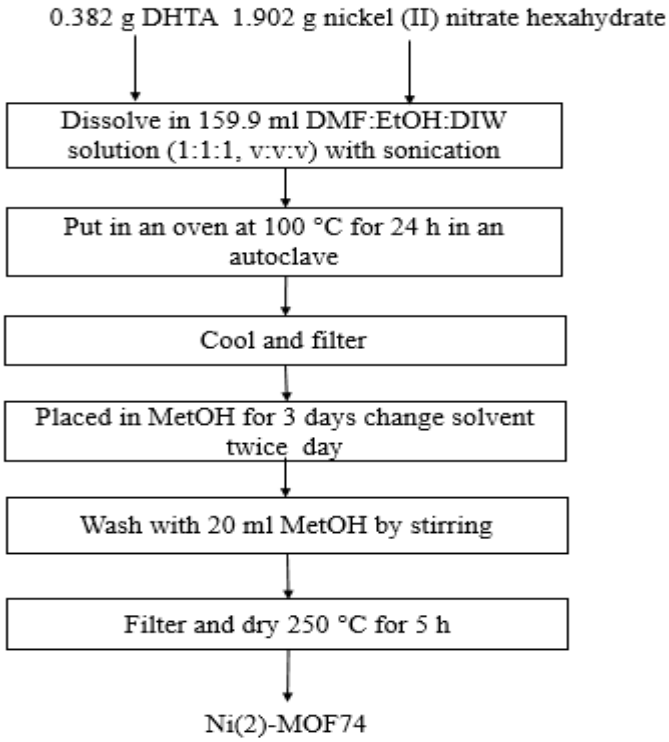

Figure 3. 4. Synthesis steps of Ni(2)-MOF74

Preparation of Ni-MOF74 at support (MOF@S);

In order to obtain Ni-MOF-74 coated zeolite 5A, modified zeolite 5A (5A(M)) was added to the sonicated solution (Wu et al. 2013).

3.2.4. Zeolitic Imidazolate Framework (ZIF8)

In this study, ZIF8 was synthesized with two different procedures and then, coated onto molecular sieve 5A (bead), alpha alumina, silica gel, molecular sieve 13X (powder) and natural zeolite clinoptilolite surfaces. Additionally, ZIF8 was deposited onto the copper based MOF.

Hydrothermal Method(ZIF8(1));

0.11 g of (0.5 mml) zinc acetate and 0.41 g of (5 mmol) 2-Methyl imidazole were placed in Teflon lined stainless steel autoclave. Then, 2 ml deionized water was added inside to the Teflon lined stainless steel autoclave. It was kept at 120 °C for 24 h. After that, it was placed in the ice bath to cool to the room temperature. It was filtered and the solid part was washed with 10 ml deionized water 3 times with centrifuge. Finally, the obtained solid was dried at 150 °C for 6 h (Lee et al. 2015)

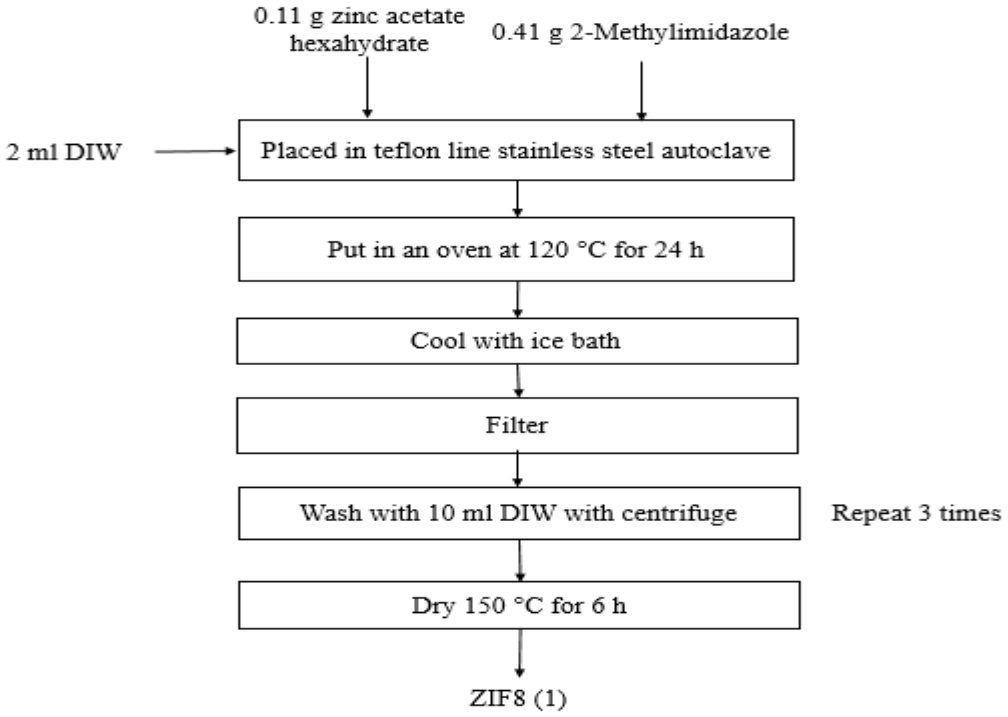

Figure 3. 5. Synthesis steps of hydrothermal method (ZIF8(1))

Solvothermal Method(ZIF8(2));

2.4 g of zinc nitrate hexahydrate was dissolved in 57 ml MeOH. At the same time, 5.3 g of 2-Methyl imidazole was dissolved in 57 ml MeOH. These two solutions were mixed and stirred for 1 h. Then it was centrifuged at 4500 rpm for 20 min. the obtained solid part was separated into two equal part and 10 ml MeOH was added to the solution for washing with centrifugation. Finally, synthesized ZIF8 was dried at 80 °C overnight.

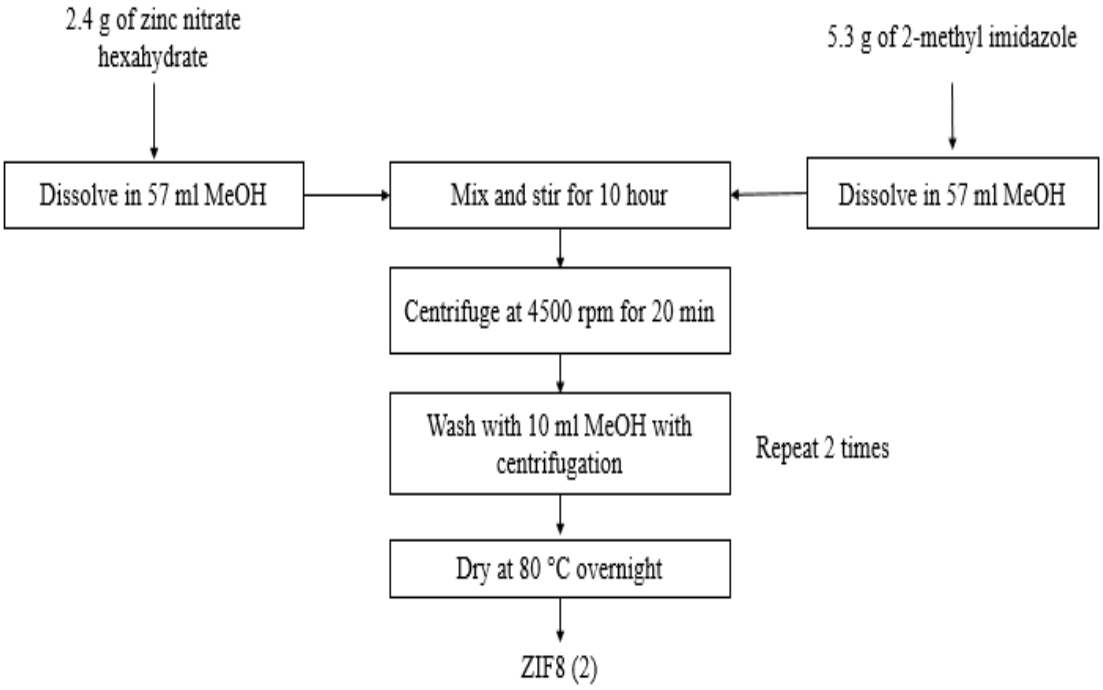

Figure 3. 6. Flow chart of solvothermal method (ZIF8(2))

ZIF8/Cu-BTC (F1, F2, F3);

A solution was prepared with 0.293 g of zinc oxide (ZnO) dispersing in 16 ml deionized water (DIW). Then, it was sonicated for 10 min. 1.74 g of $Cu(NO_3)_2.3H_2O$ and 16 ml DMF was added to this solution by stirring. At the same time, 0.84 g of trimesic acid and desired amount of Imi (Imi: H_3BTC, 1:1, 1:2, 1:3, w: w) was dissolved in 16 ml EtOH. Later on, prepared solutions were mixed for one min at room temperature and filtered. The solid part was washed with 50 ml EtOH for 3 times. Finally, the obtained solid was dried under vacuum at 120 °C for 6 h (Li et al. 2017).

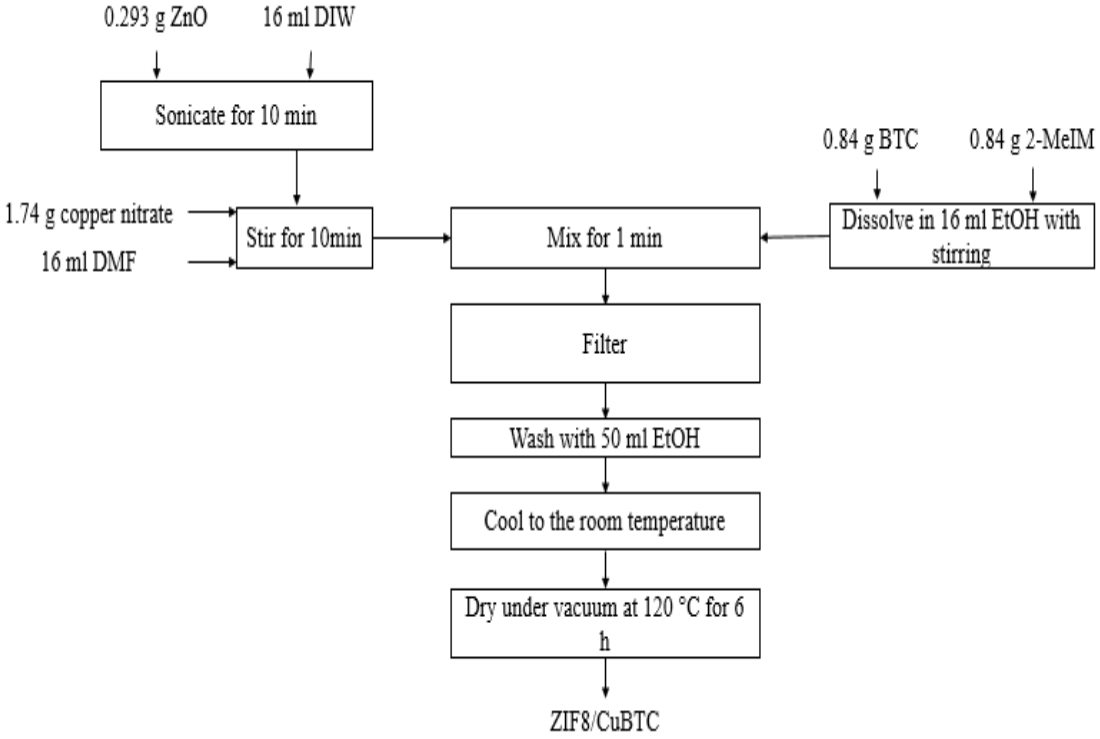

Figure 3. 7. Flow chart of ZIF8/Cu-BTC (F1, F2, F3)

3.3. Coating of the support surface

Modified or seeded support surface were coated with metal organic framework(Ni-MOF-74, ZIF8, CuBTC and ZIF8). The seeded clinoptilolite surface was coated with CuBTC and ZIF8 (F1@CLN(S), F2@CLN(S), F3@CLN(S)). The raw clinoptilolite surface was coated with solvothermal synthesized ZIF8 (ZIF8(S)@CLN). The modified 5A was coated with Ni based organic framework(Ni(1)@M(5A) or Ni(2)@M(5A)).

In direct synthesis support materials was added to the MOF solution at the beginning of the synthesis. Then synthesis procedure of MOF was followed step by step.

3.4. Characterization Studies

Characterization study of this thesis was done by using the XRD, ATR-IR, SEM, UV-vis and UV-ISR.

X-Ray Diffraction (XRD)

The crystalline structures of the catalysts were determined by Philips X'Pert diffractometer with CuKα radiation. The scattering angle 2θ was varied from 5 ° to 50 °, with a step length of 0.02.

Attenuated Total Reflectance (ATR-IR)

Functional groups present on the materials were analyzed between 650-4000 cm^{-1} with ATR-IR (Pelkin Elmer).

Scanning Electron Microscope (SEM)

Surface morphology of the materials were investigated by SEM, EDX, and mapping analysis with FEI QUANTA 250 FEG model.

UV-ISR

Band gap energies of the materials were determined by UV-ISR spectrophotometer. The analysis was performed by using Shimadzu UV-ISR 2600.

Band gap calculation formulas are given below.

$$hv = \frac{1240}{wavelength}$$

$$\alpha = \frac{(1 - reflectance)^2}{2 * reflectance}$$

$$y - axis = (hv * \alpha)^2$$

CHAPTER 4

RESULTS AND DISCUSSION

In this study, the effect of surface treatment of the support materials on the coating of the MOF was examined. Molecular sieve 5A (5A), alpha alumina (α), silica gel (SG), molecular sieve 13X (13X) and natural zeolite mineral clinoptilolite (CLN) were chosen as support material and nickel based MOF (Ni-MOF74), zeolitic imidazole framework (ZIF8) and combination of ZIF8 and CuBTC were employed as the coating materials. The band gaps of these composite materials was also tested.

4.1. MOF synthesis

In this study Ni- and Zn- based organic frameworks were synthesized and called as Ni-MOF74 and zeolitic imidazole framework (ZIF8), respectively.

Synthesis of CuBTC and ZIF8

ZIF8(F2) with 2:1 (trimesic acid to imidazole ratio) has the peaks around 7° and 12.5° in comparison with the ratio 1:1 and 3:1. Moreover, it has a higher intensity than other fast synthesized ZIF8(F1) and with the 1:1 and 3:1 trimesic acid to imidazole ratio.

ATR-IR spectrum of this method is given in Figure 4.2. Peaks at 728 cm^{-1}, 1370 cm^{-1}, 1653 $cm^{-1,}$ and around 3300 cm^{-1} refer to C=C bending, C-H bending, C=C stretching and O-H stretching, respectively. The carboxylic group which comes from trimesic acid form the peak of O-H stretching around 3300 cm^{-1}.

CuBTC and ZIF8 composites were synthesized with different ratios of organic ligands (H_3BTC:Imi, 1:1, 2:1, 3:1). According to SEM microgram, this composite does not have significant crystal structures. In spite of that increasing H_3BTC amount creates clear cubic structures which are seen in Figure 4.3. However, the same defects are observed on the surface of the composed crystals (Li et al. 2017).

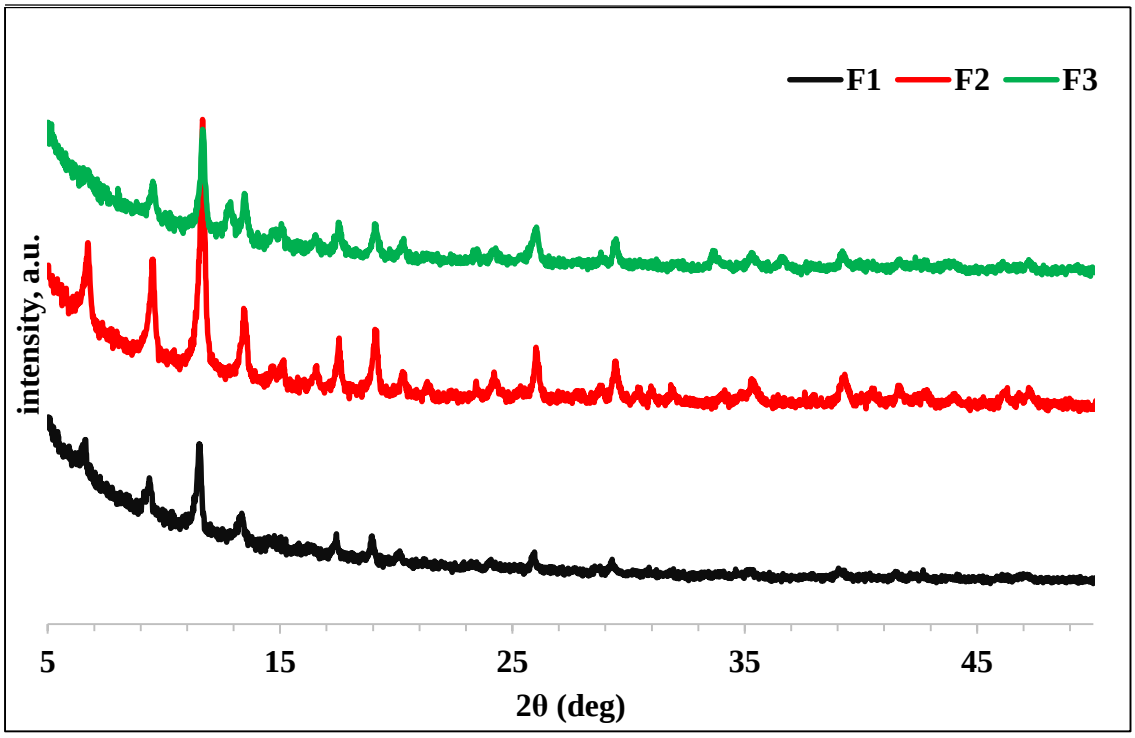

Figure 4. 1. XRD pattern of F1, F2, F3

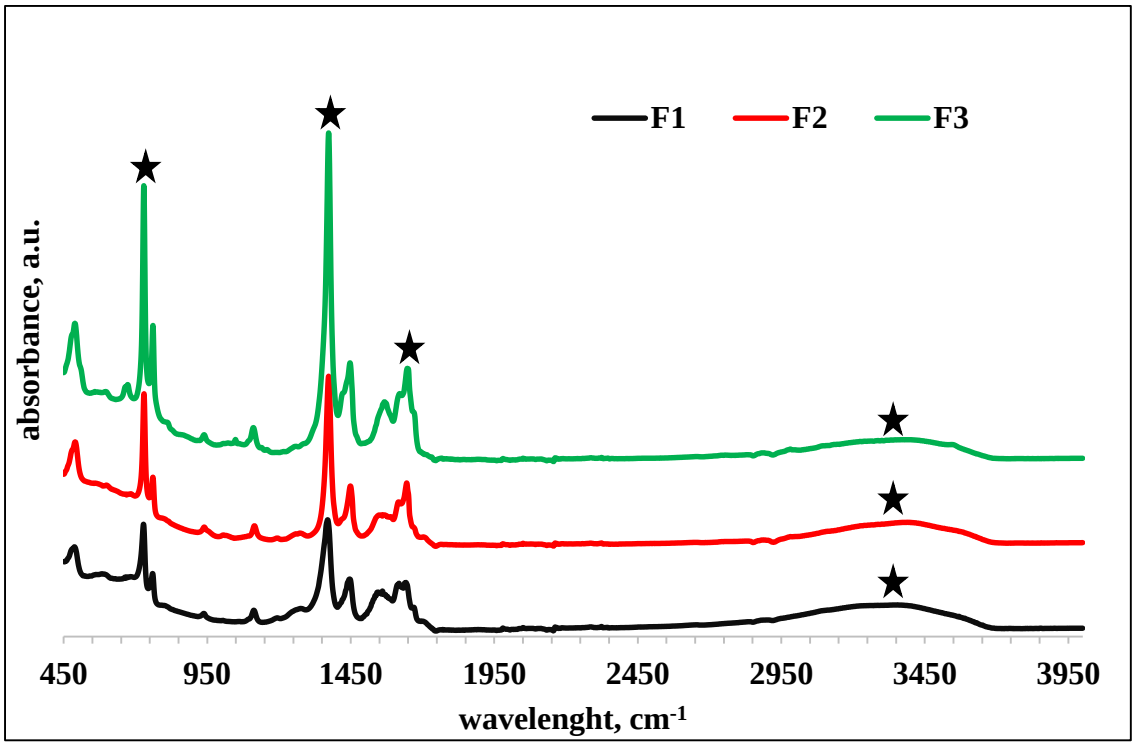

Figure 4. 2. ATR-IR spectrum of F1, F2 and F3

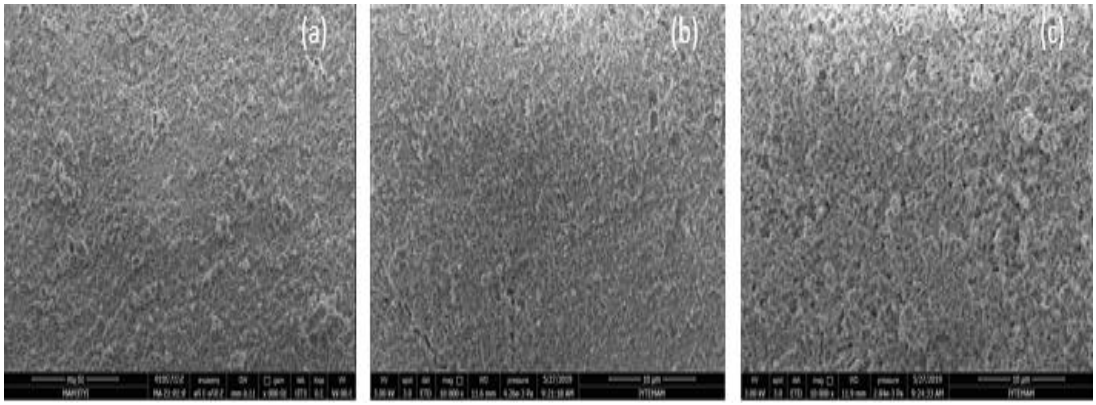

Figure 4. 3. SEM images of F1 (a), F2 (b) and F3 (c)

Effect of Synthesis method on ZIF8

ZIF8 was synthesized according to two different procedure which was hydrothermal (ZIF8(1)) and solvothermal method (ZIF8(2)) (Keser Demir et al. 2014).

XRD patterns of ZIF8 materials are shown in Figure 4.4. The characteristic peaks (2θ) of ZIF8 around 7°, 10°, 12.5°, and 17° are observed for both of them as observed in the literature (Lee et al. 2015).

Figure 4.5 shows that ATR-IR spectrums of ZIF8(1) and ZIF8(2). The peak around 3300 cm^{-1} does not appear. Unlikely, peak around 1147 cm^{-1} in the dry-gel method belongs to C-O stretching. Peaks at 696 cm^{-1} and 760 cm^{-1} refer to the C=C stretching vibration in the ZIF8s. It was found that ZIF8(1) and ZIF8(2) have the same characteristic peaks of 2-Methylimidazole and trimesic acid (Li et al. 2017).

Figure 4.6. shows that SEM images of ZIF8(1) and ZIF8(2). ZIF8(1) has more crystalline structure than ZIF8(2). In spite of that ZIF8(2) has more dense texture with smaller crystals.

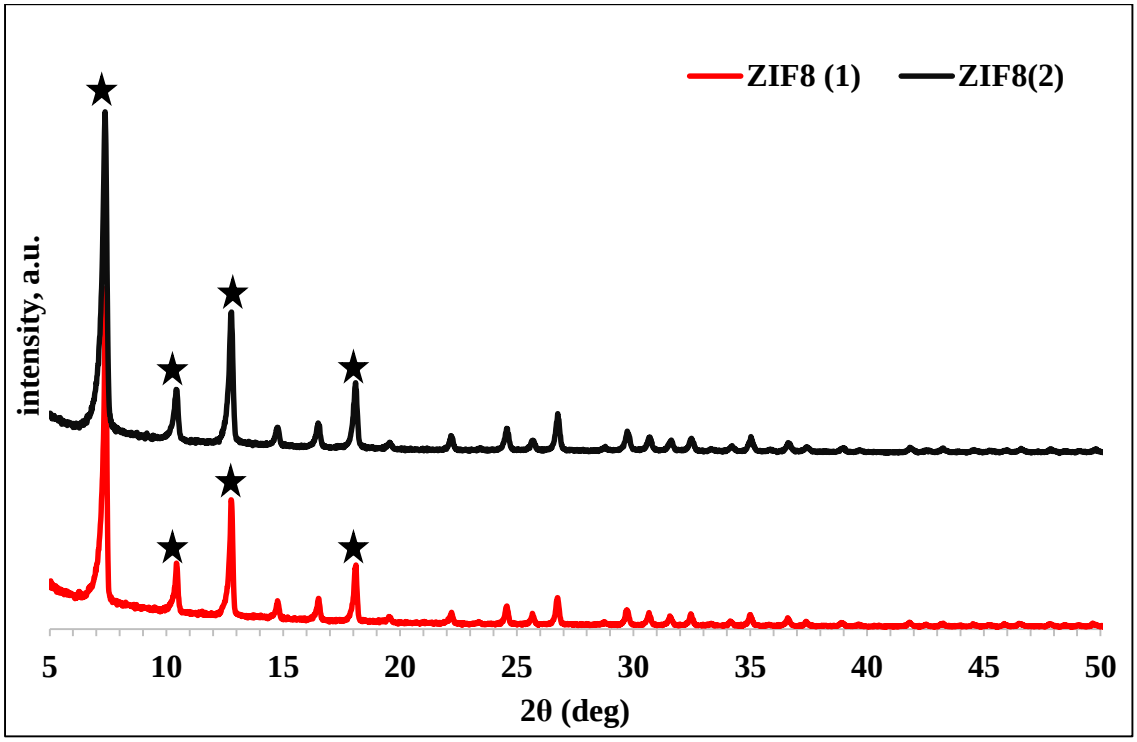

Figure 4. 4. XRD pattern of ZIF8(1) and ZIF8(2)

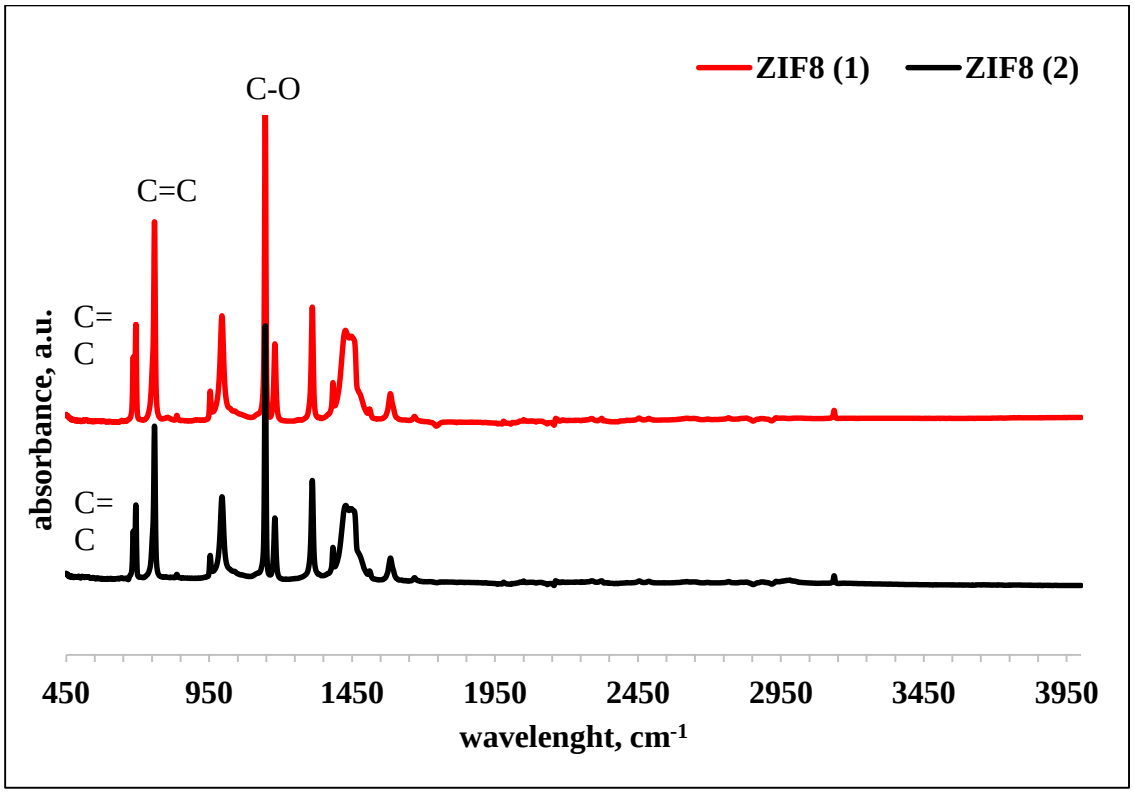

Figure 4. 5. ATR-IR spectrum of ZIF8(1) and ZIF8(2)

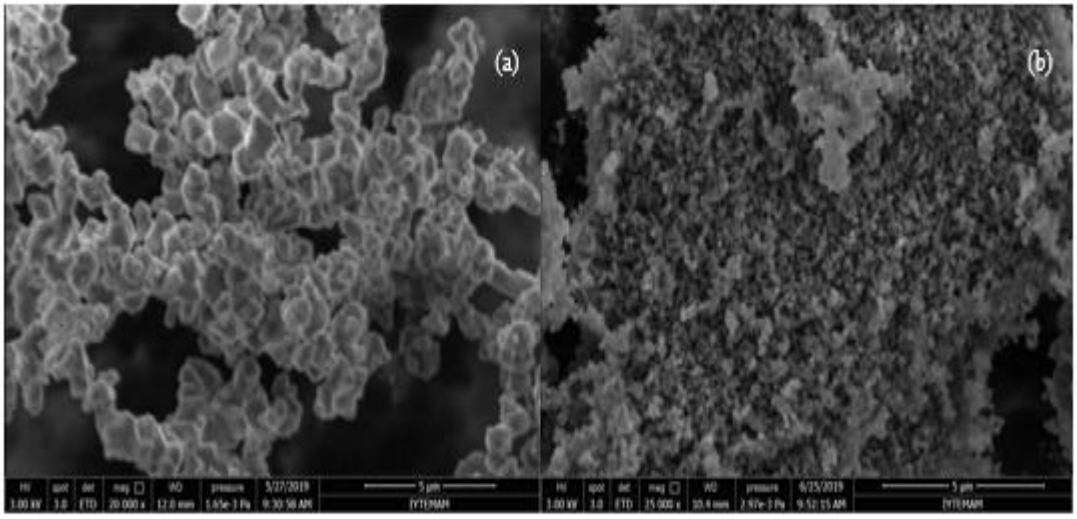

Figure 4. 6. SEM images of ZIF8(1) (a) ZIF8(2) (b)

4.2. Surface treatment of support material

The surface of the support material is modified with APTES or MOF seeding method. To understand the effect of the APTES modification ZIF8 was coated also the untreated clinoplilolite (CLN).

APTES modification(M);

XRD patterns of zeolite 5A and modified zeolite 5A (5A(M)) are shown in Figure 4.6. Characteristic peaks of 5A were observed at 2θ= 10, 12.5, 16, 27 and 34.5° was observed for both of them showing them this modification was not changed the cristalinity of the 5A.

During this modification -COOH groups were attached on the surface of zeolite 5A (Al-Naddaf, Thakkar, and Rezaei 2018). In order to understand the functional group formation on the surface of the zeolite 5A, C=O and O-H peaks should be observed at 1380 cm^{-1} and 1560 cm^{-1}, respectively. As seen in Figure 4.7. the expected peaks do not observe and the functional groups do not form with APTES modification on the zeolite 5A beads.

According to SEM micrograph, bare zeolite 5A has the crystalline structure. Surface modification of zeolite 5A with succinic anhydride and APTES causes crystals to enlarge shown in Figure 4.8. Fractures are observed on the treated zeolite surfaces. Al-Naddaf et al. applied the surface treatment method onto zeolite 5A. They observed that

modification of zeolite surface with succinic anhydride and APTES causes to form bigger crystals (Al-Naddaf, Thakkar, and Rezaei 2018).

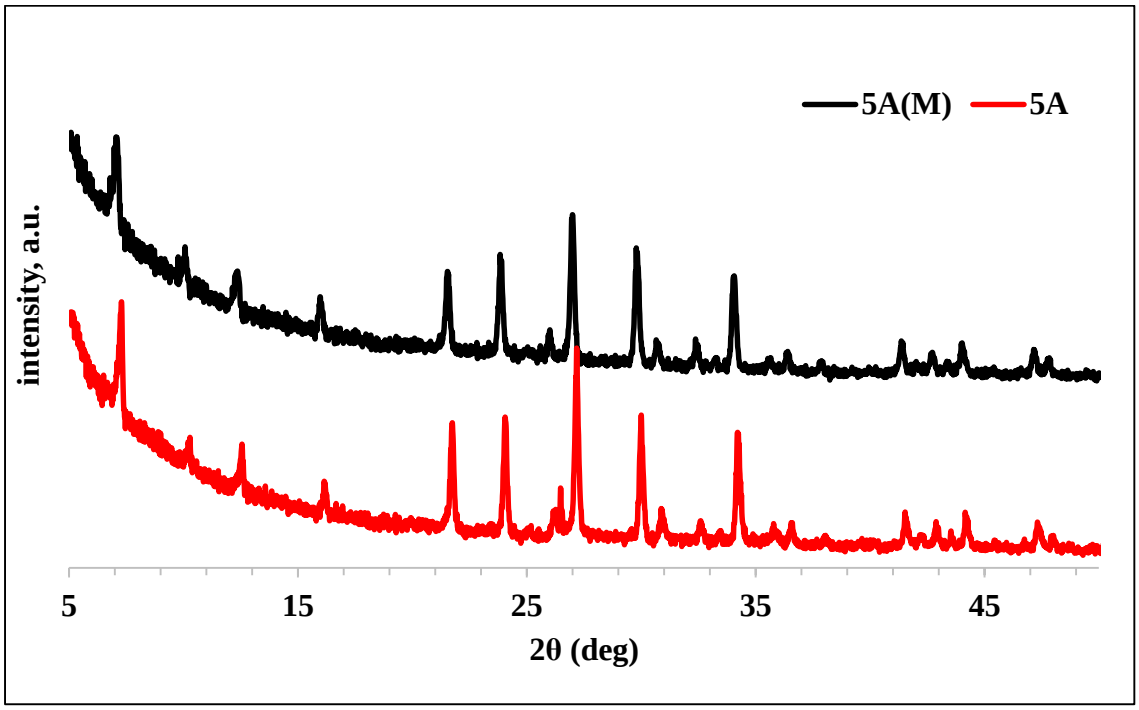

Figure 4. 7. XRD pattern of zeolite 5A (5A) and APTES modified zeolite 5A (5A(M))

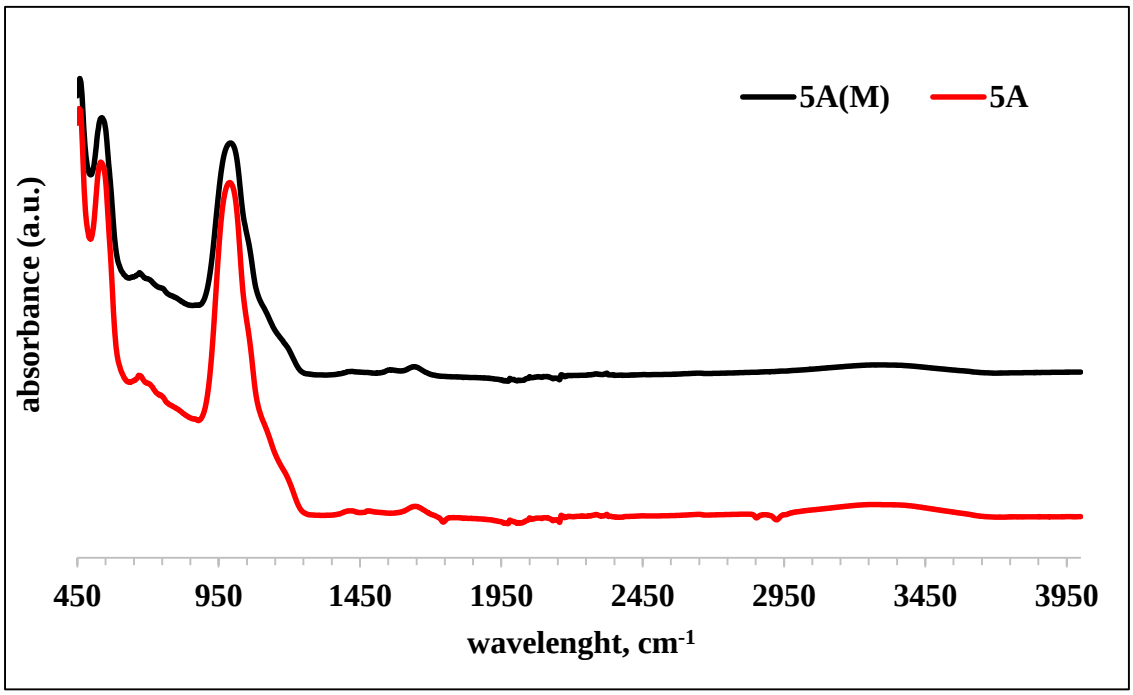

Figure 4. 8. ATR-IR spectra of zeolite 5A (5A), APTES modified zeolite 5A (5A(M))

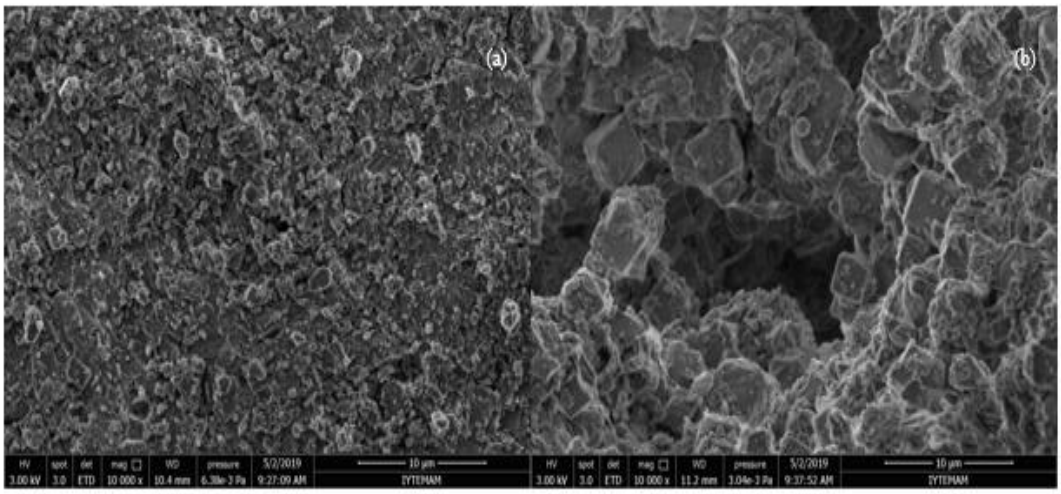

Figure 4. 9. SEM images of zeolite 5A (a) and 5A(M) (b)

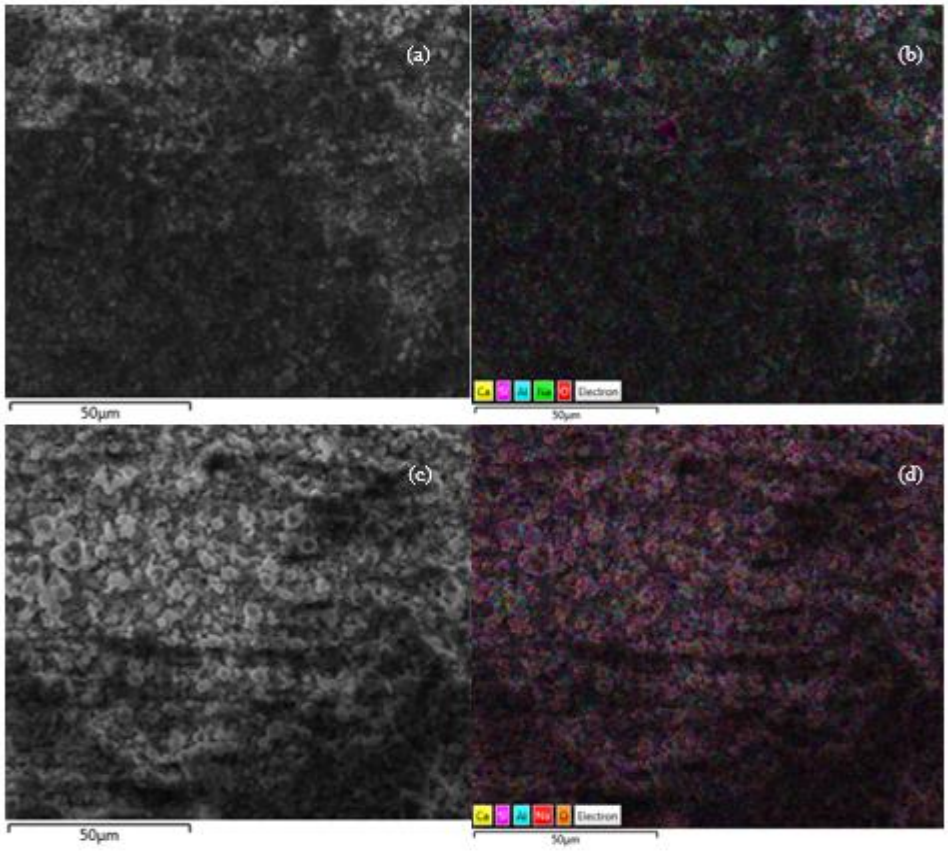

Figure 4. 10. SEM and EDX mapping analysis of 5A((a) and (b)) and 5A(M)((c) and (d))SEM and EDX mapping of 5A((a) and (b)) and 5A(M)((c) and (d))

Elemental analysis gives information about chemical composition of surface of materials. It is expected that carboxylic acid groups are formed in the surface of zeolite 5A. Increasing oxygen amount shows the carboxylic acid formation on the surface.

Table 4.1. Elemental analysis of 5A and treated 5A

	5A		5A(M)	
Element	Wt%	Atomic%	Wt%	Atomic%
O	53.00	66.51	54.26	67.67
Na	3.21	2.81	3.42	2.97
Al	19.15	14.25	18.03	13.33
Si	19.15	13.69	18.52	13.16
Ca	5.49	2.75	5.77	2.87
Total:	100.00	100.00	100.00	100.00

This modification was applied onto the surface of α-alumina (α), zeolite 13X (13X) and clinoptilolite (CLN) and the XRD and ATR-IR plots were presented in Figure 4.9-4.14, repectively. There is no difference between bare and modified supports. This means APTES modification does not cause any change in the crystal and chemical structure of the supports.

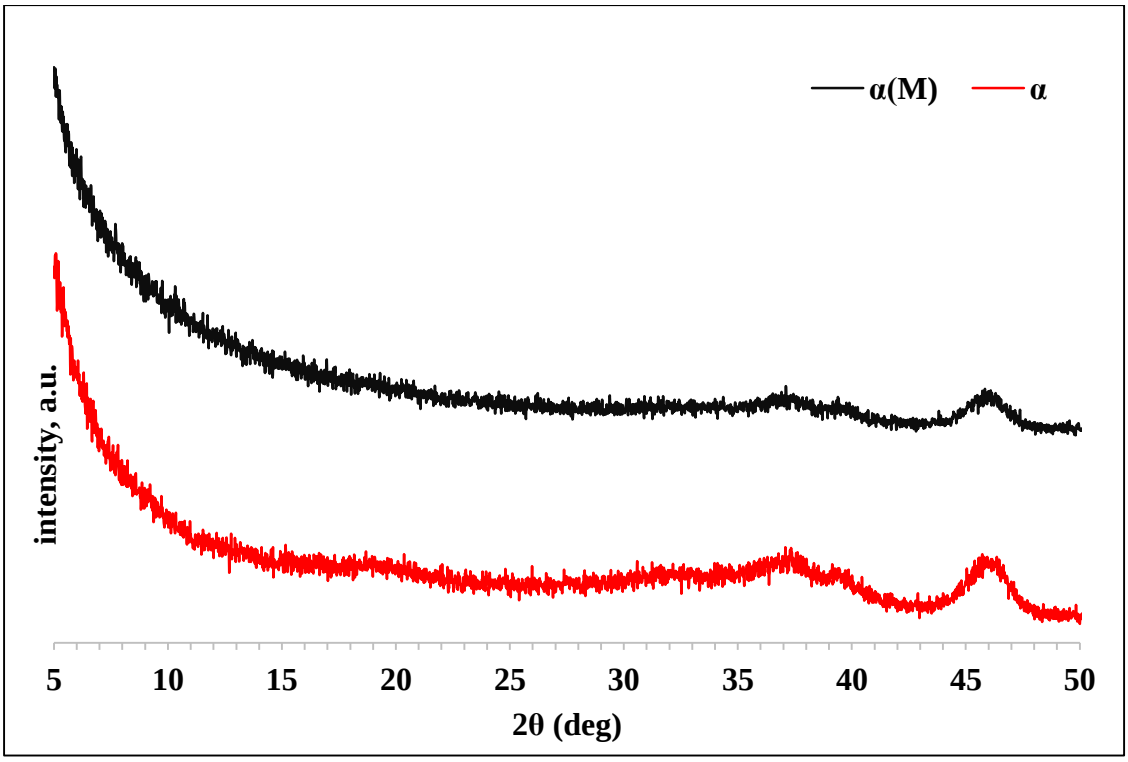

Figure 4. 11. XRD pattern of alpha alumina (α) and APTES modified alpha alumina (M(α))

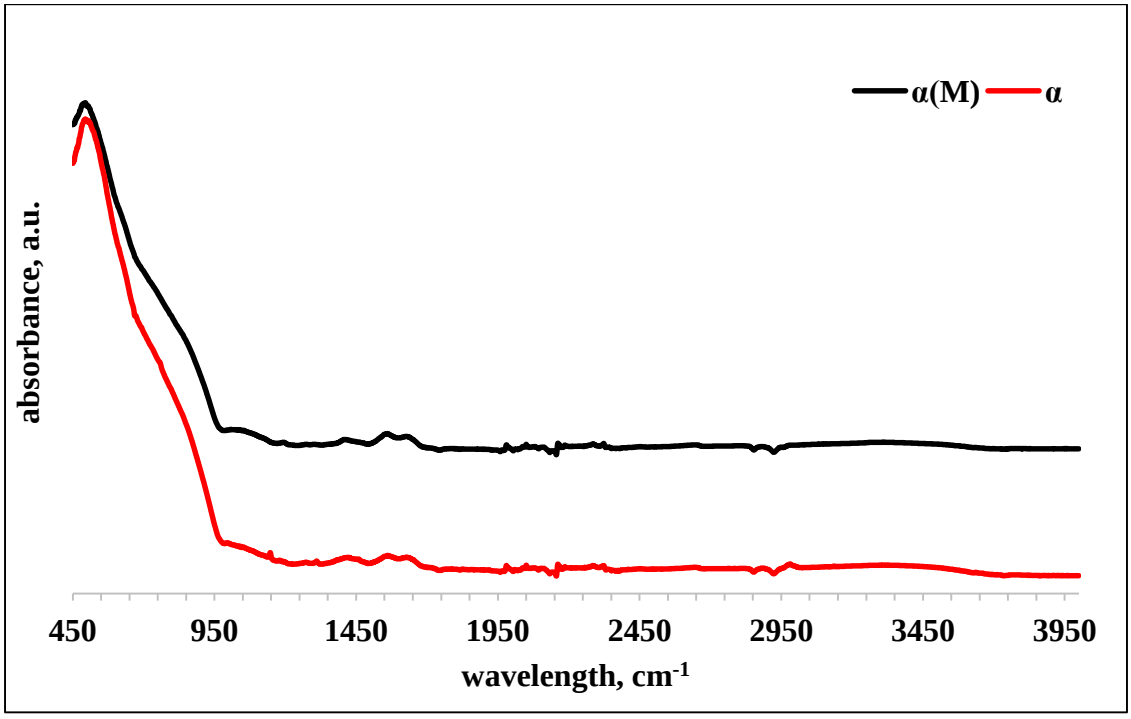

Figure 4. 12. ATR-IR spectra of alpha alumina (α) and APTES modified alpha alumina (M(α))

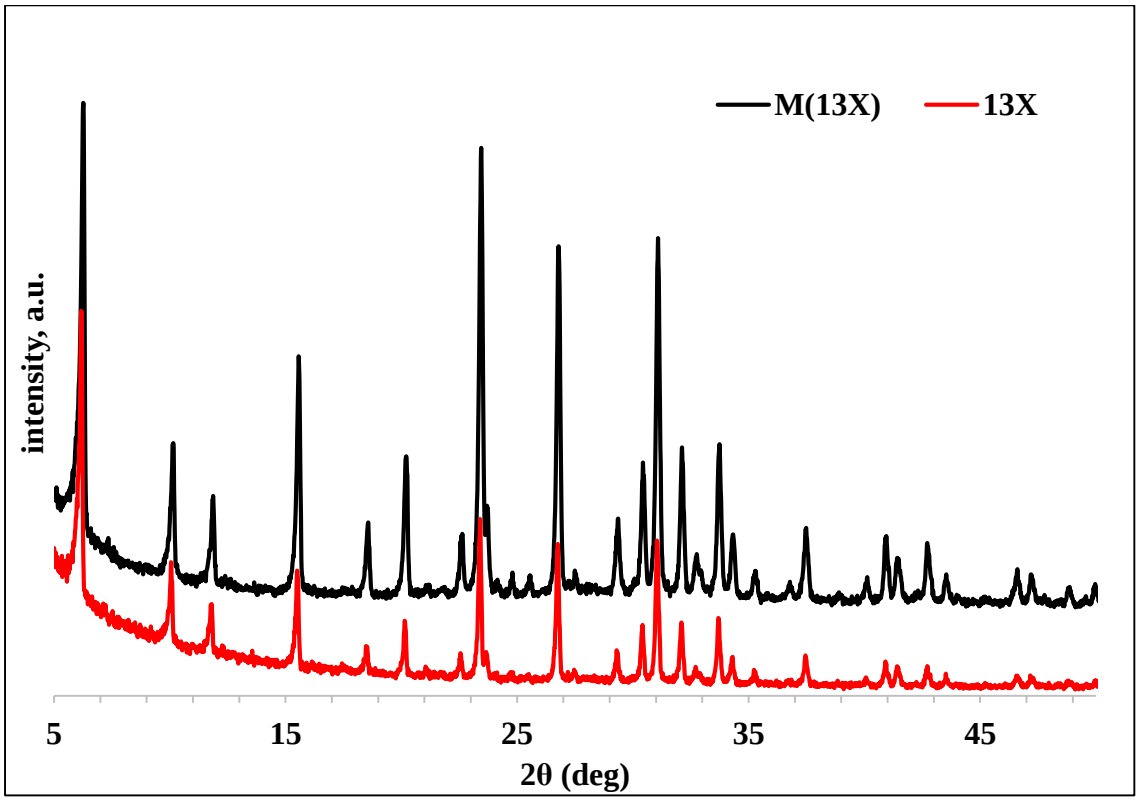

Figure 4. 13. XRD pattern of 13X and APTES modified 13X (13X(M))

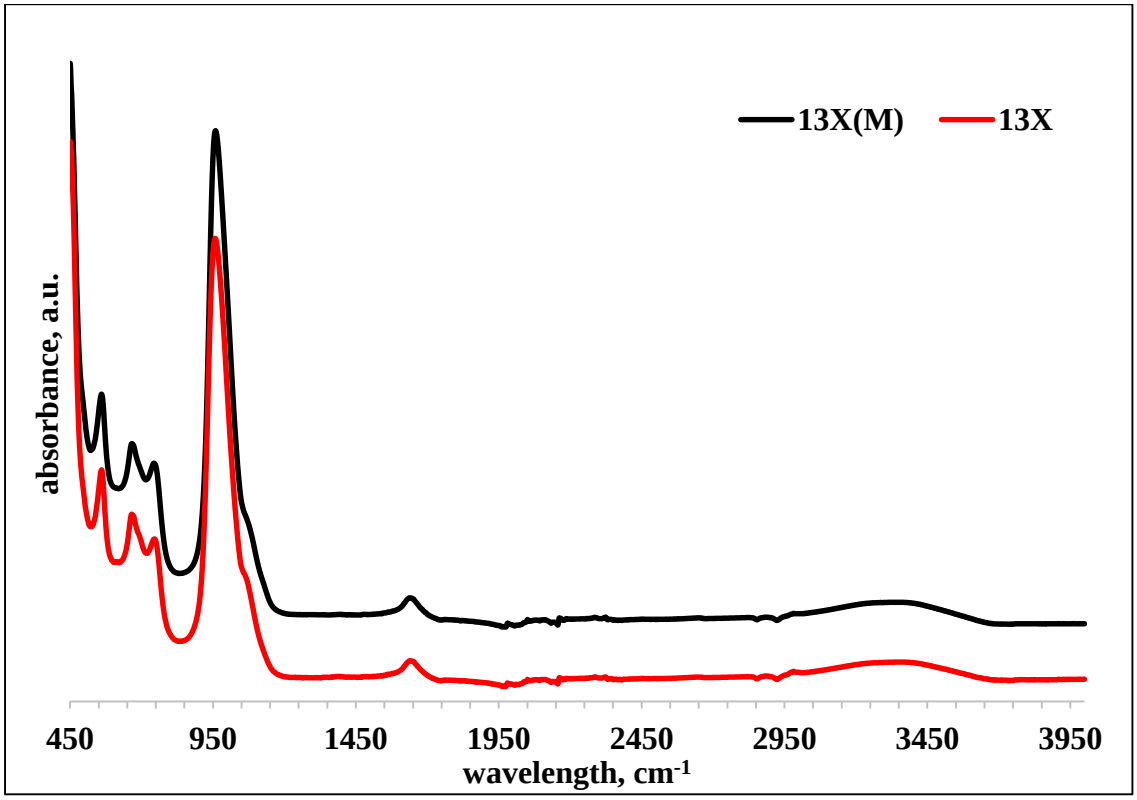

Figure 4. 14. ATR-IR spectra of 13X powder and APTES modified 13X powder

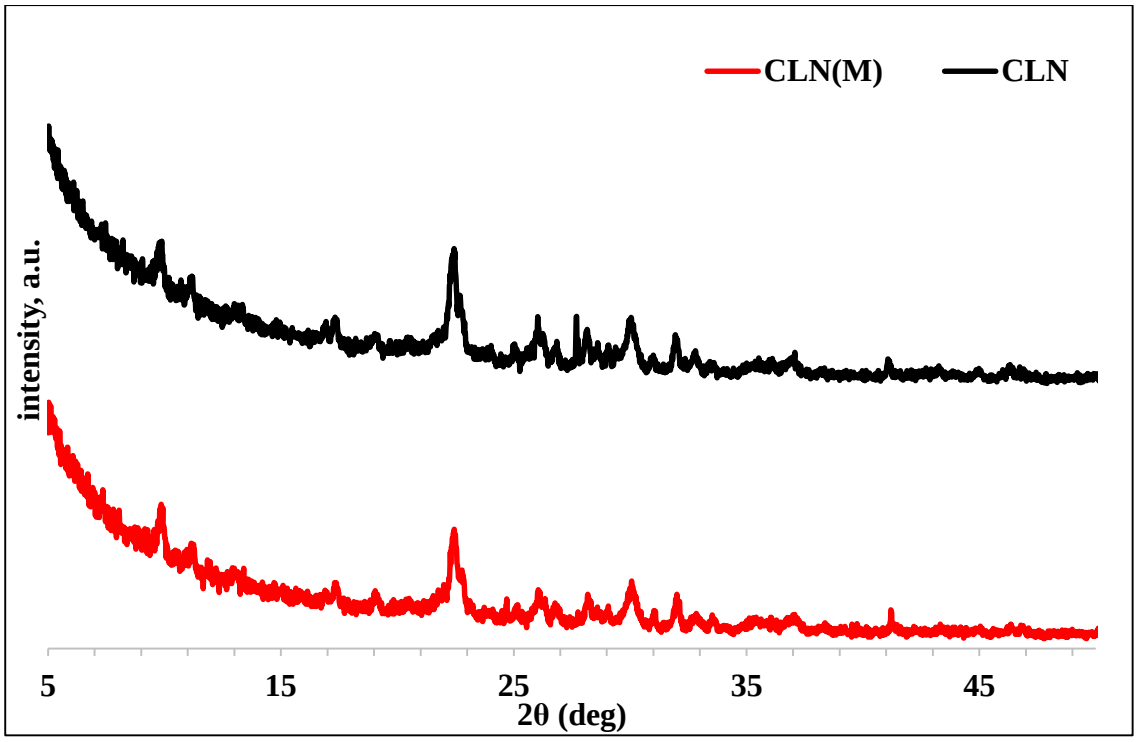

Figure 4. 15. XRD pattern of clinoptilolite (CLN) and APTES modified clinoptilolite (CLN(M))

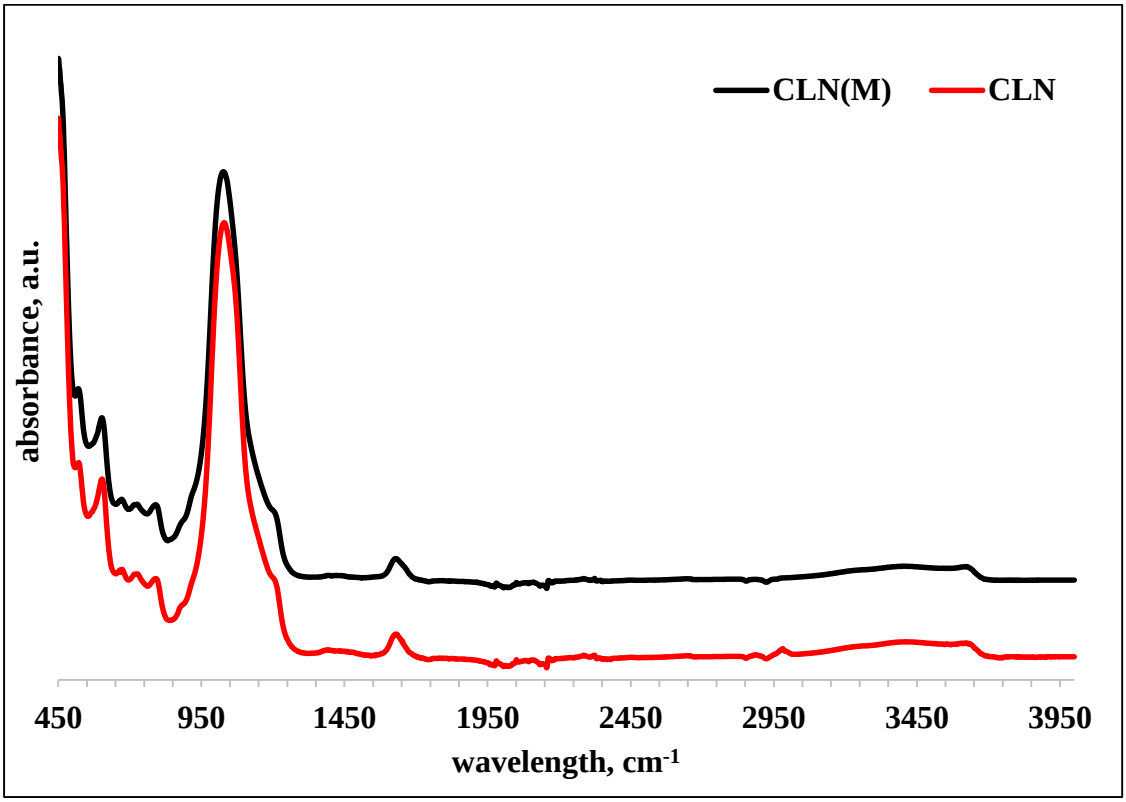

Figure 4. 16. ATR-IR spectra of clinoptilolite (CLN) and APTES modified clinoptilolite (CLN(M))

Seeding method(S);

Seeding method was applied to the surface of support material to prepare this material for coating with MOFs. Tate et al. studied with seeding of MOF onto the zeolite 5A beads. They used Al-MOF for the seeding procedure (Tate et al., 2016). Instead of this Ni- and Zn- based organic frameworks were produced. Then seeding method was applied onto the support surfaces with these MOF crystals.

After synthesis of F1, F2 and F3 crystals, the seeding procedure was applied onto the clinoptilolite (CLN). Figure 4.15 and 4.16 are the XRD pattern and ATR-IR spectrum of (5A). The X-Ray diffraction main peaks expected at 2θ= 7°, 9°, 12°, 19°, and 25° are observed at 6.59°, 9.42°, 11.54°,19.01° and 26°.

Additionally, functional groups were analyzed with ATR-IR analysis (Figure 4.16). The seeded cl has the main peak of zeolite at 1045 cm^{-1} which belongs to C-O stretching. Besides, the formation of C=C bending at 746 cm^{-1} and medium O-H bending at 1371 cm^{-1} are observed. These functional groups come from MOF crystals.

In addition to this seeded zeolite has similar peaks of bare zeolite at around 2θ= 9.9°. 23°, 26°, 30°, and 32°. Also, seeded zeolite should have the property of MOF crystals and bare zeolite. According to figure seeded zeolite sample has the peaks around 2θ= 9.92°, 11.27°, 22.49°, 26.13°, and 30.12°. This result shows that the seeded sample has a crystal structure similar to bare zeolite and MOF crystals.

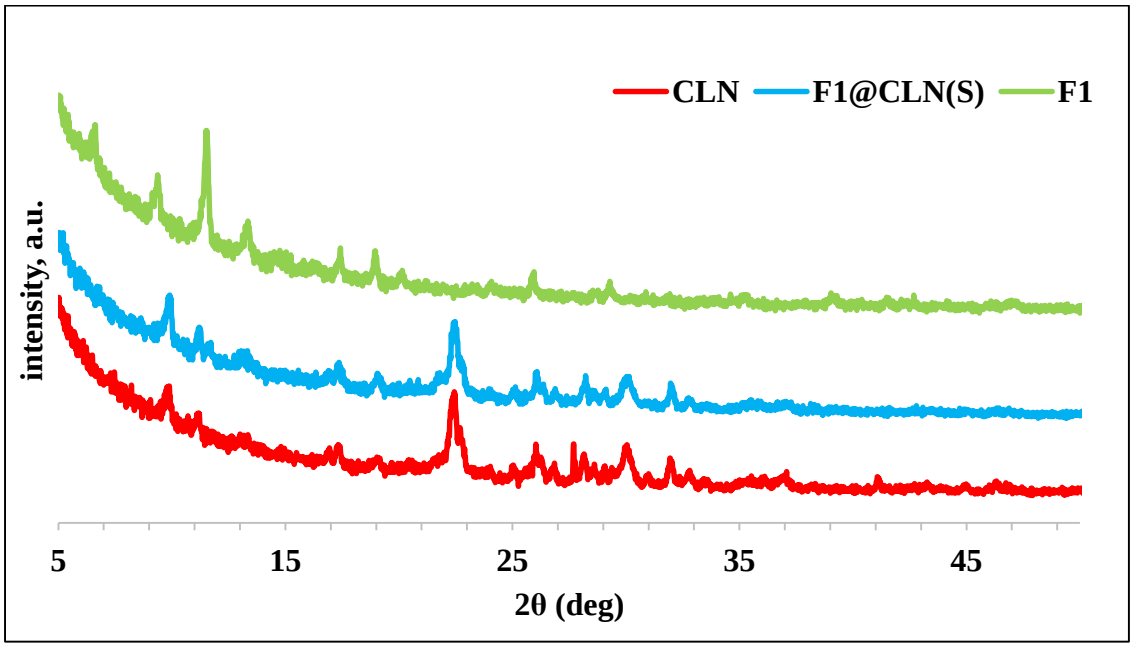

Figure 4. 17. XRD patterns for CLN-based F1 composites

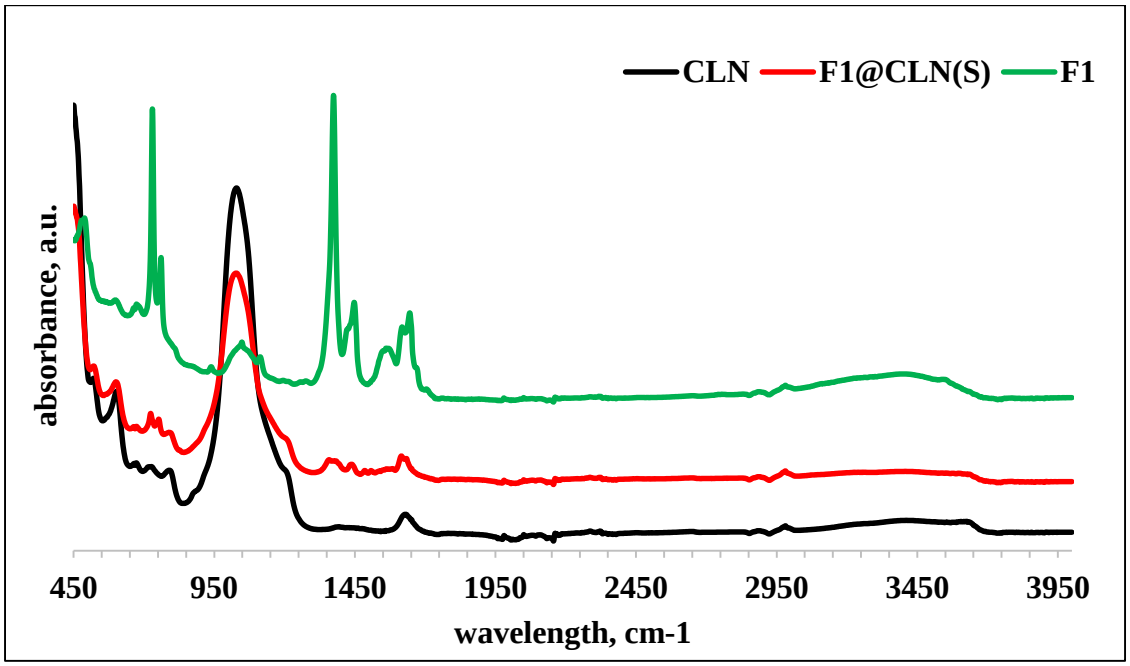

Figure 4. 18. ATR-IR spectrum for CLN-based F1 composites

Figure 4.17 and 4.18 are the XRD pattern and ATR-IR spectrum of powder zeolite MOF crystals with 2:1 BTC to imidazole ratio and seeded zeolite with this MOF. F2 MOF gives the same results with F1 MOF. It has the main peaks 2θ= 9.54°, 11.66°, 17.52°, and

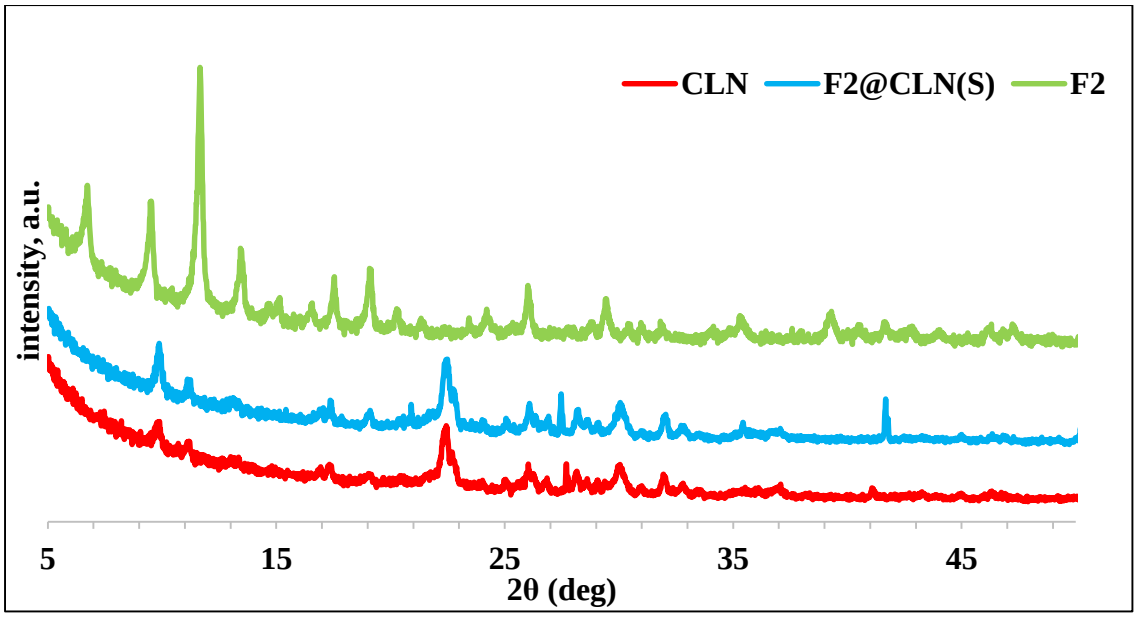

Figure 4. 19. XRD patterns for CLN-based F2 composites

19.09°. Solely, higher intensities are seen in figure 4.11 than figure 4.9. This can be explained with bigger crystals formed in the MOF F2 with 2:1 BTC to imidazole ratio. Furthermore, seeded zeolite with F2 crystals has the main peaks both bare zeolite and MOF.

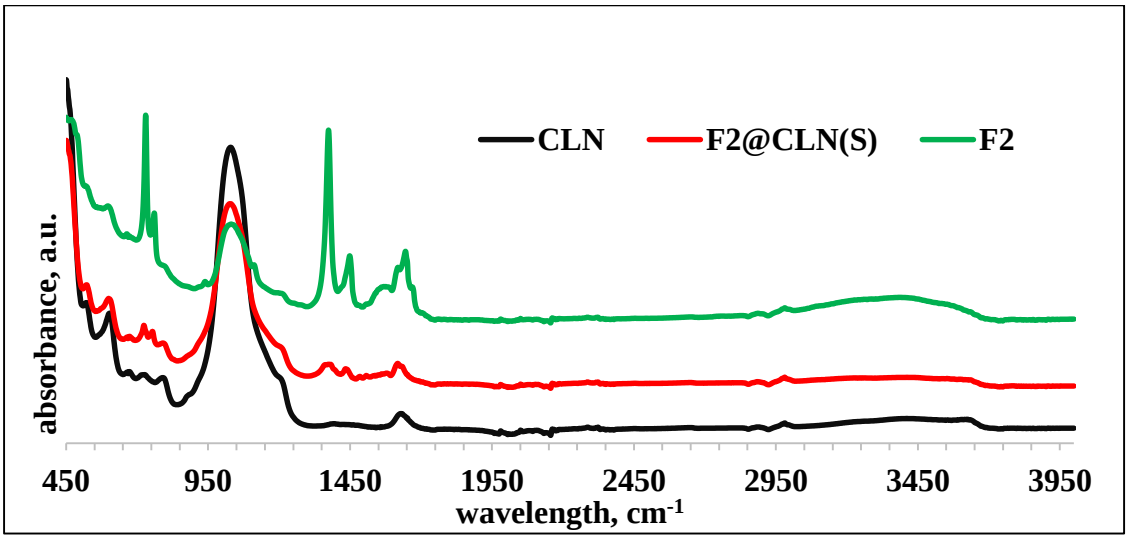

Figure 4. 20. ATR-IR spectrum for CLN-based F2 composites

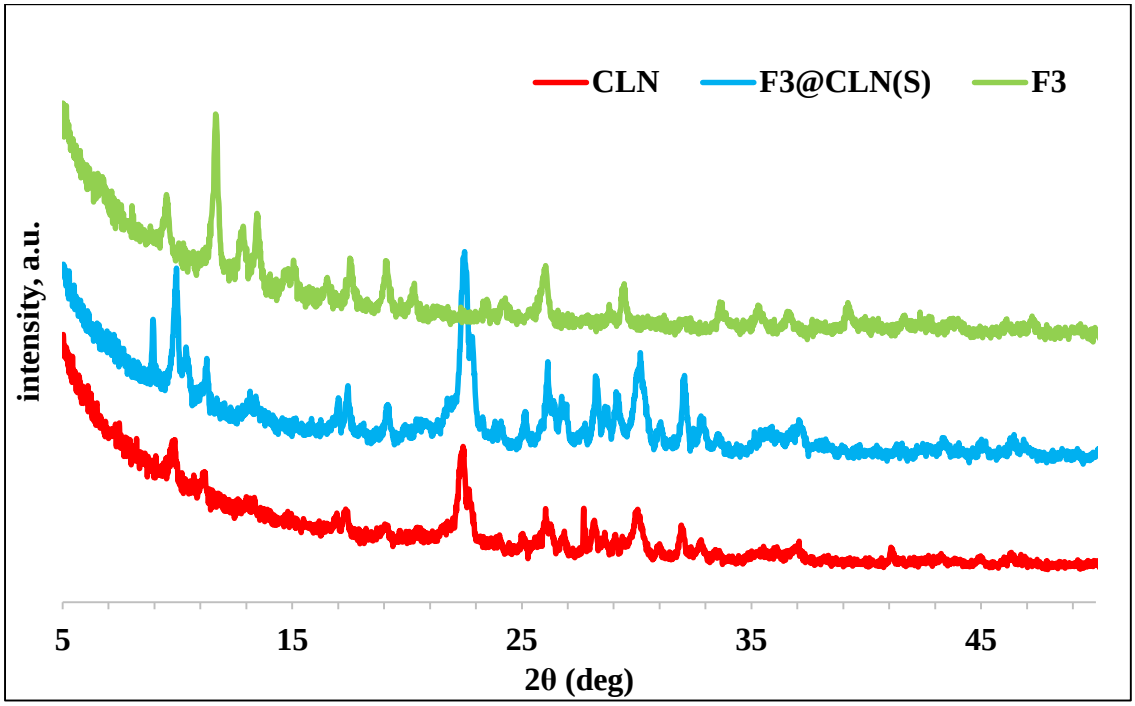

Figure 4. 21. XRD patterns for CLN-based F3 composites

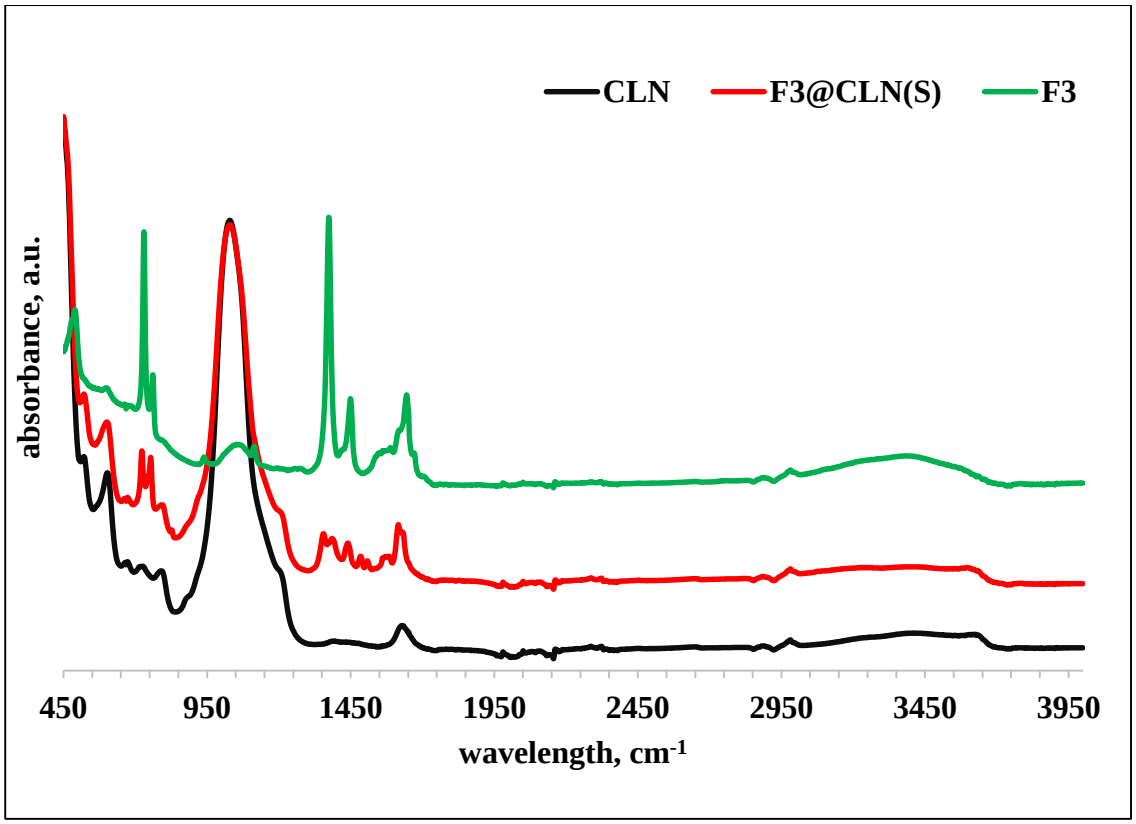

Figure 4. 22. ATR-IR spectrum for CLN-based F3 composites

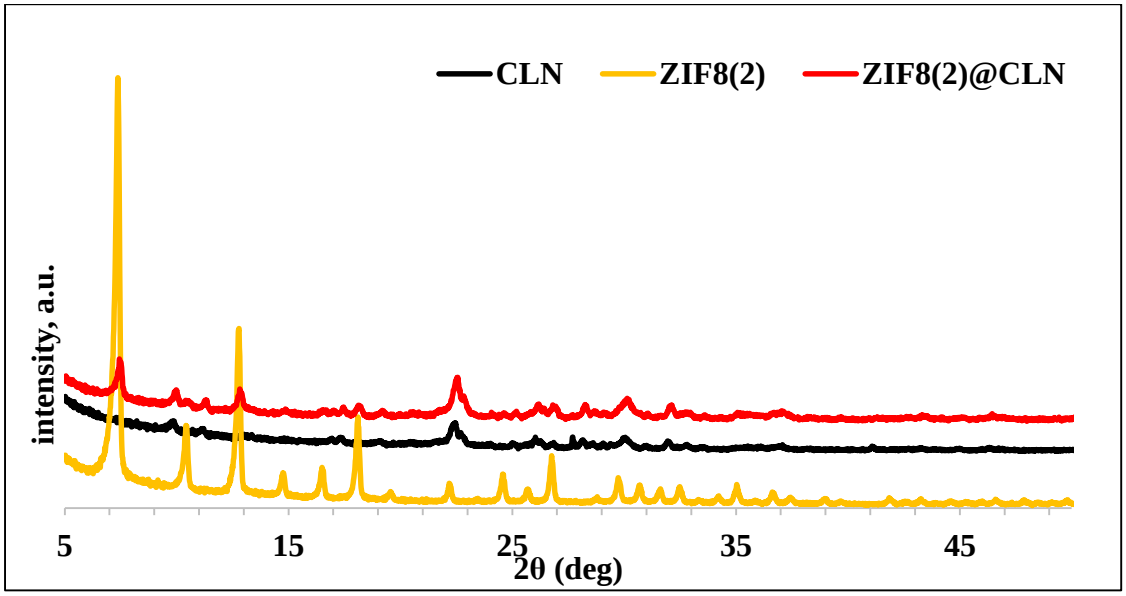

Figure 4. 23. XRD patterns for clinoptilolite ZIF8(2) composite

4.3. Coating of support surfaces

Modified (M), seeded(S) and untreated support surfaces coated with ZIF8 and Ni-MOF74 and F. Effect of seeding method were investigated by analyzing seeded and non-seeded supports.

Figure 4.23. Shows the XRD pattern of untreated clinoplilolite (CLN), ZIF8(2) and their composite. The ZIF8 main peaks at 2θ= 7.32° and 12.83° and clinoptilolite main peak at 22.5 and 30.16° are clearly observe in the composite.

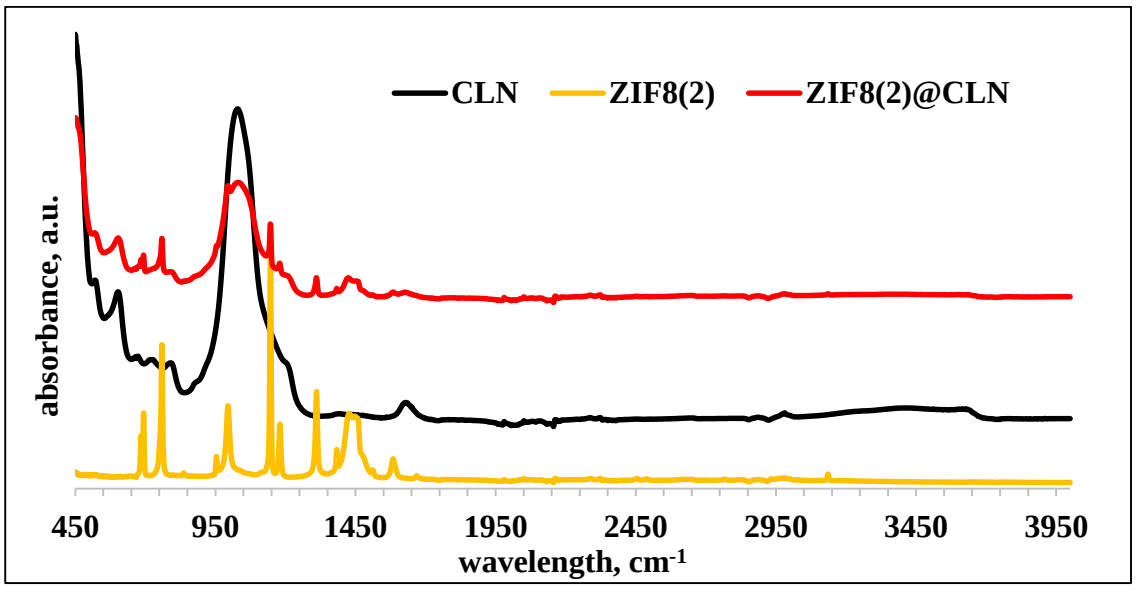

Figure 4. 24. ATR-IR spectra for clinoptilolite ZIF8(2) composite

The composite material has the strong C-H bending and C-O stretching at 760 cm^{-1} and 1148 cm^{-1} which belongs to the ZIF8 besides to the tedrahedral stretching(O-T-O) at 1000 cm-1 and 608 cm-1 of clinoptilolite (Figure 4.22).

Figure 4.23. shows SEM images of the solvathermally synthesized ZIF8 and ZIF8,CLN composite and images of the composite. As seen from the Fig. nano size ZIF8 was synthesized and these spherical structures are syhetized in the CLN particle. Also, mapping analysis shows Zn- hold on to the CLN.

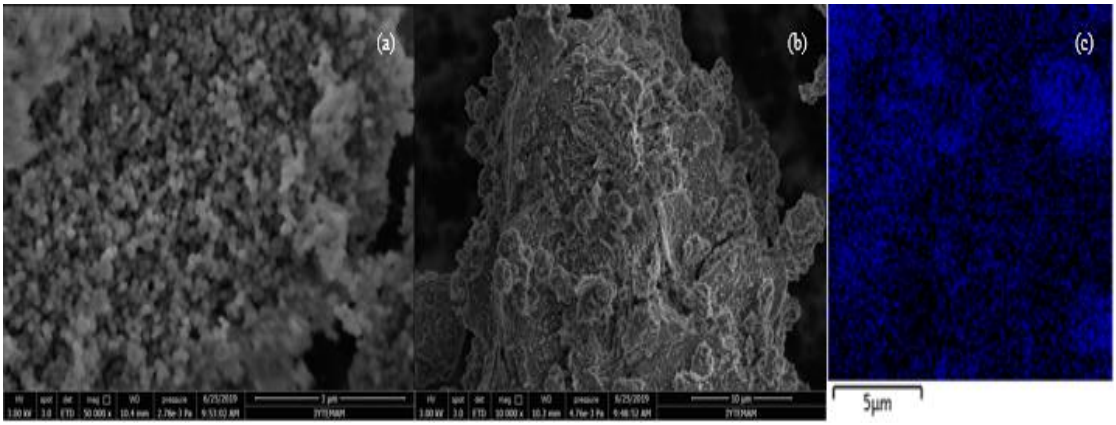

Figure 4. 25. SEM images of ZIF8(2) (a), ZIF8(2)@CLN (b) and mapping analysis of ZIF8(2)@CLN (c)

Figure 4.24. shows that the diffraction pattern of 5A, modified zeolite 5A (M5A) and Ni-MOF74 coated zeolite 5A(Ni@M5A). It can be seen that Figure 4.24. nickel coated M5A (Ni@M5A) has the same characteristic peaks at (2θ=7°, 10°, 12.5°, 16°, 27°, and 34.5°) with M5A. (Al-Naddaf, Thakkar, and Rezaei 2018). Coated zeolite 5A has a peak at 7.58° in this study. It shows that the crystal structure of zeolite 5A does not change. Moreover, nickel MOF is coated successfully on the surface of the zeolite and reactor walls. Besides, peak intensities of synthesis in schott bottle are the higher than Ni-MOF-74@M5A synthesized in an autoclave. Thus, bigger crystals are formed in the schott bottle.

It can be seen in Figure 4.24. nickel based metal organic framework coated modified 5A has the characteristic peaks around 570 cm^{-1} and 1000 cm^{-1}. Additionally, a new peak is observed around 1600 cm^{-1}. Al Naddaf et al. studied with the modification and coating of zeolite 5A surface with nickel based MOF and the characteristic peaks of modified and coated 5A were observed at 1100 cm^{-1} and 1650 cm^{-1} (Al-Naddaf, Thakkar, and Rezaei 2018). The results of this study are in consistence with the literature.

Peaks around 500 cm^{-1} refer to Si-O and Si-O-Si which comes from zeolite 5A structure. Peaks at 1000 cm^{-1} and 1600 cm^{-1} belong to C-O stretching and C=C stretching, respectively.

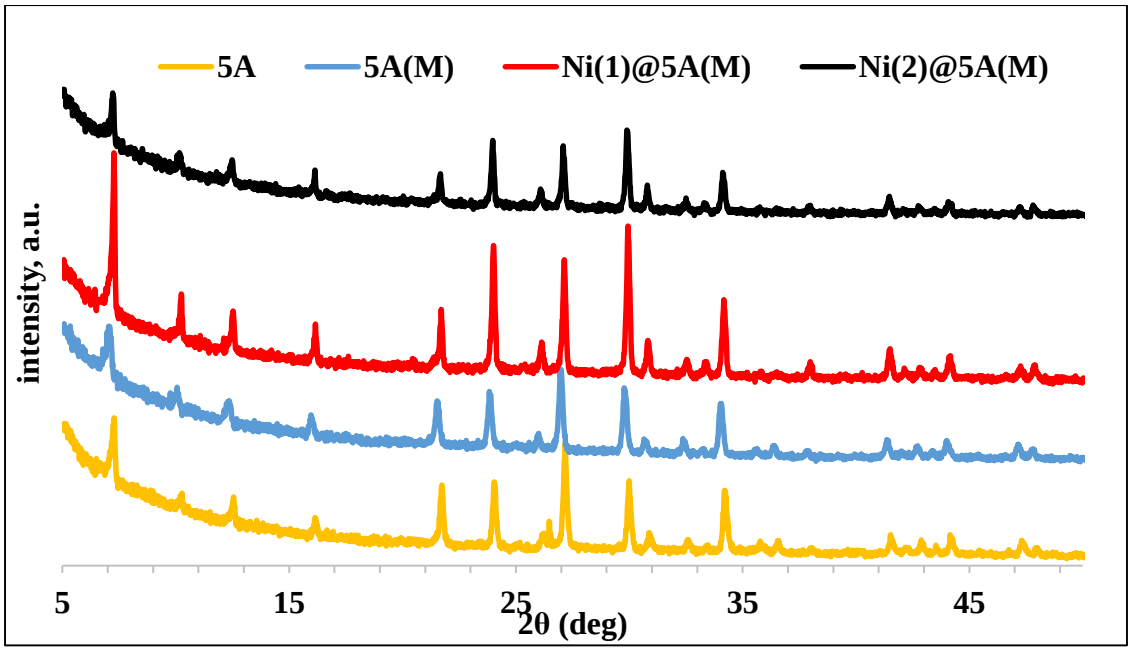

Figure 4. 26. XRD pattern of zeolite 5A based composite

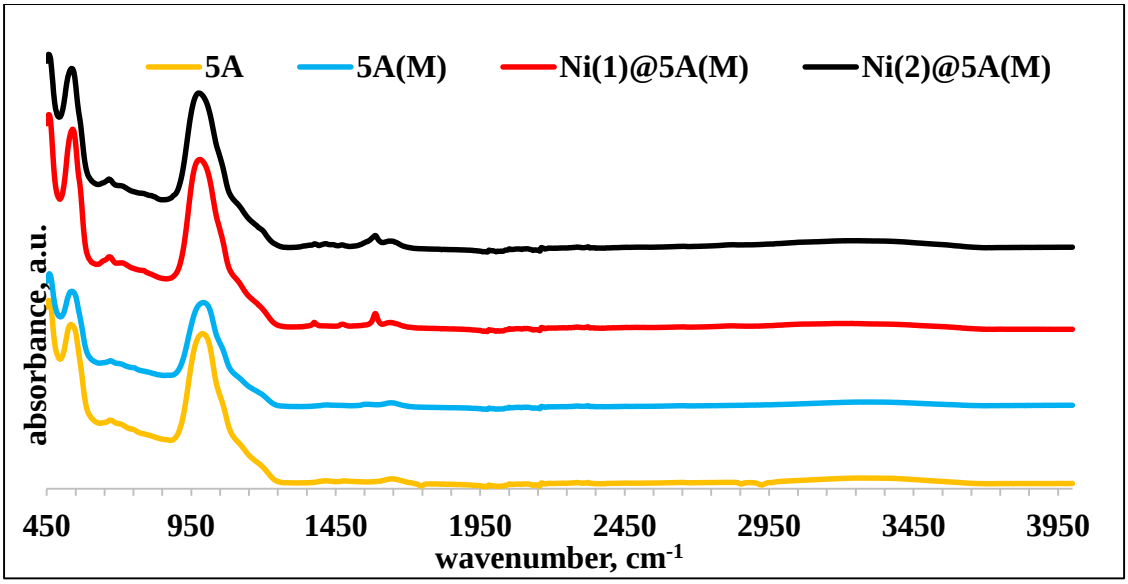

Figure 4. 27. ATR-IR spectra of 5A, modified 5A (M5A), nickel MOF coated modified 5A (Ni-MOF-74(1)@M5A and nickel MOF coated modified 5A (Ni-MOF-74(2)@M5A

While treating and coating with MOF synthesized using nickel nitrate is shown in Figure 4.12 and treating and coating with MOF synthesized using nickel acetate is shown in Figure 4.13. Surface modification of zeolite 5A with succinic anhydride and APTES causes defects on the surface and these defects filled by coating with Ni-MOF-74. MOF crystal is obviously seen on the coated surface of the zeolite.

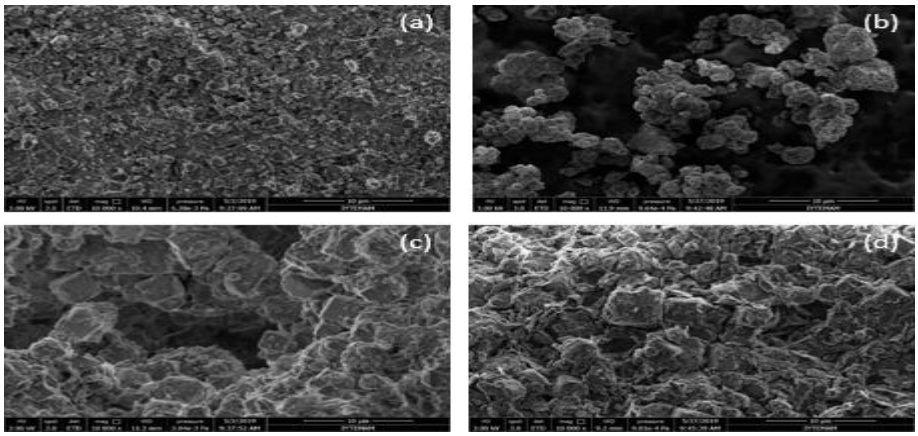

Figure 4. 28. SEM images of bare zeolite 5A (a), surface modified zeolite 5A (5A(M)) (b), Ni-MOF74 (c) and Ni-MOF74@5A(M) (d)

Band Gap Analysis

Band gap energy is obtained from the plots given below. After UV-DSR analysis, calculations is done according to formulas given in section 3.4. Then band gap energies are obtained. Band gap energies are listed in table 4.2.

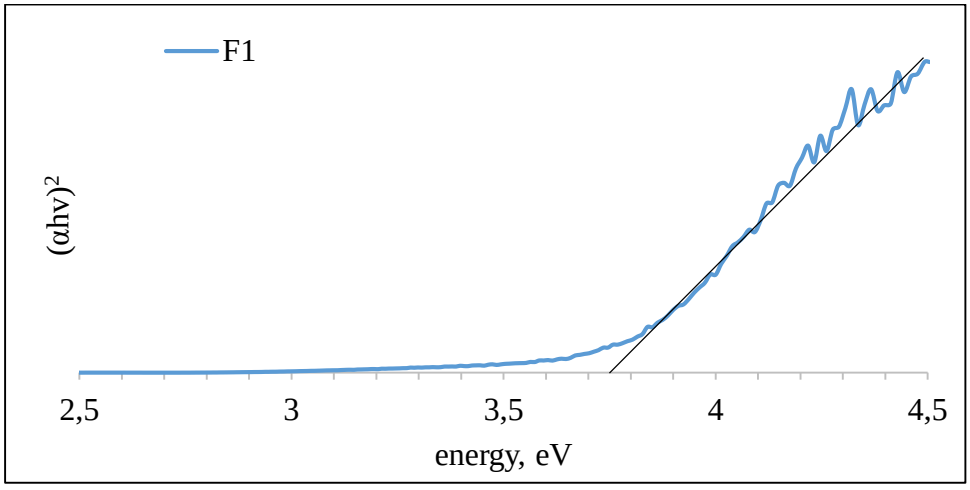

Figure 4. 29. Energy band gap plot of F1

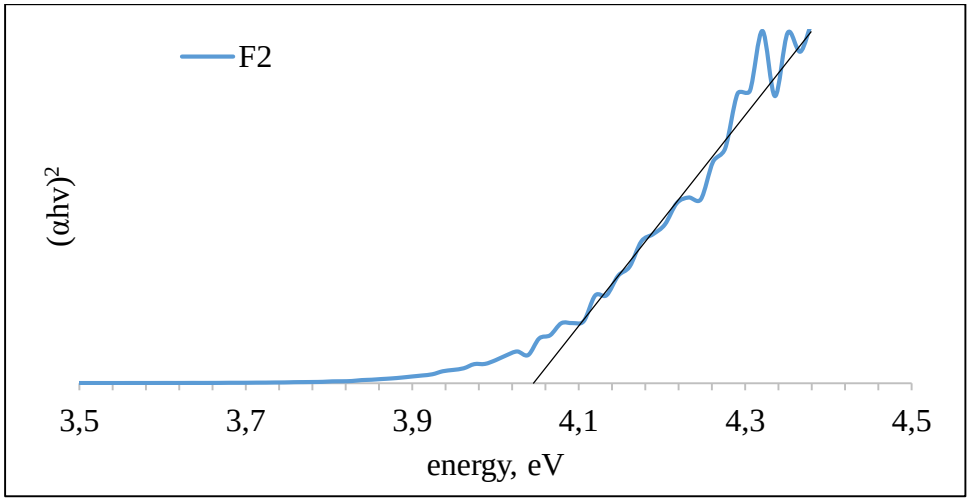

Figure 4. 30. Energy band gap plot of F2

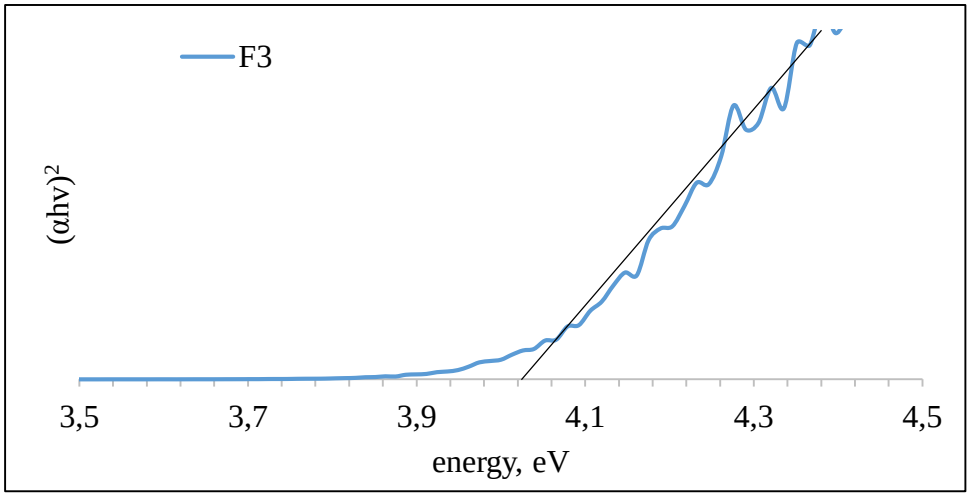

Figure 4. 31. Energy band gap plot of F3

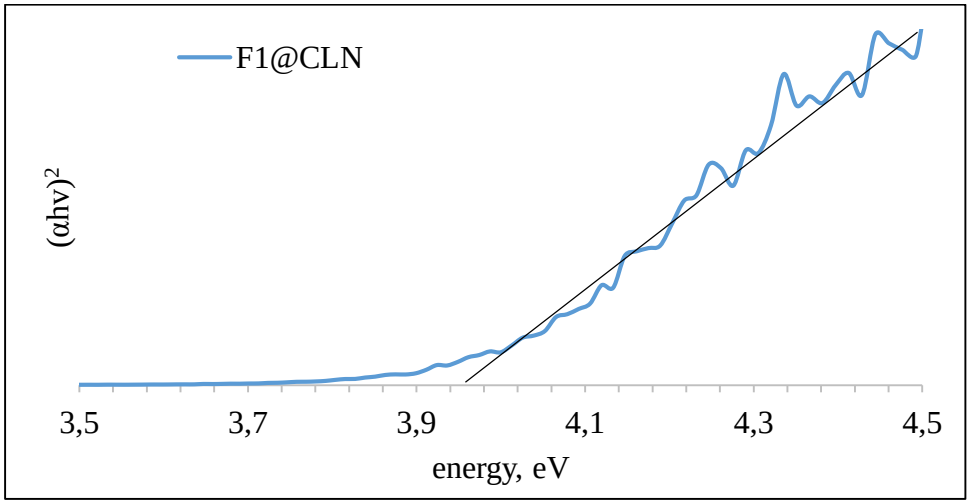

Figure 4. 32. Energy band gap plot of F1@CLN

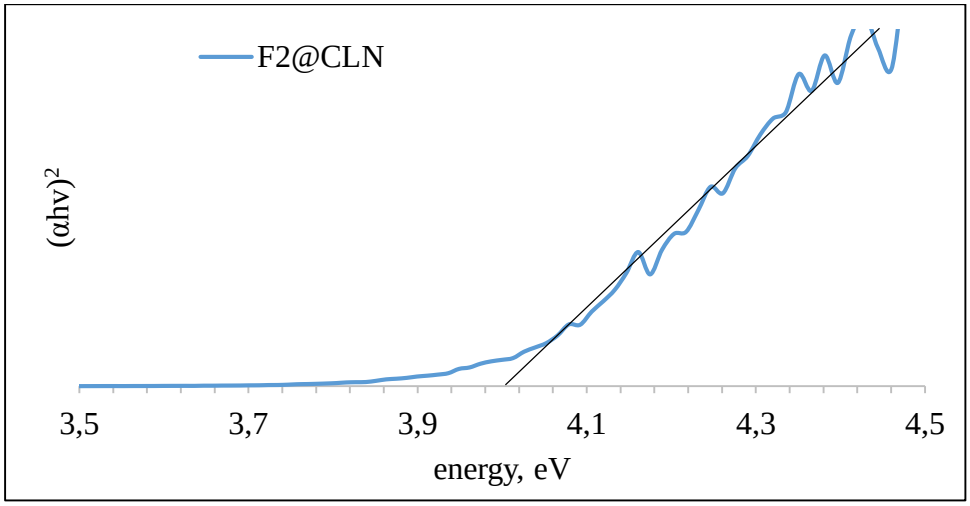

Figure 4. 33. Energy band gap plot of F2@CLN

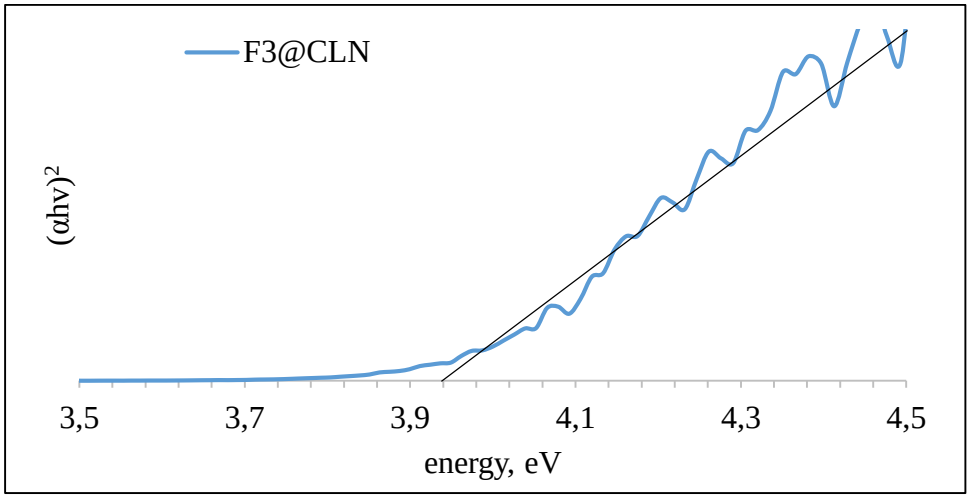

Figure 4. 34. Energy band gap plot of F3@CLN

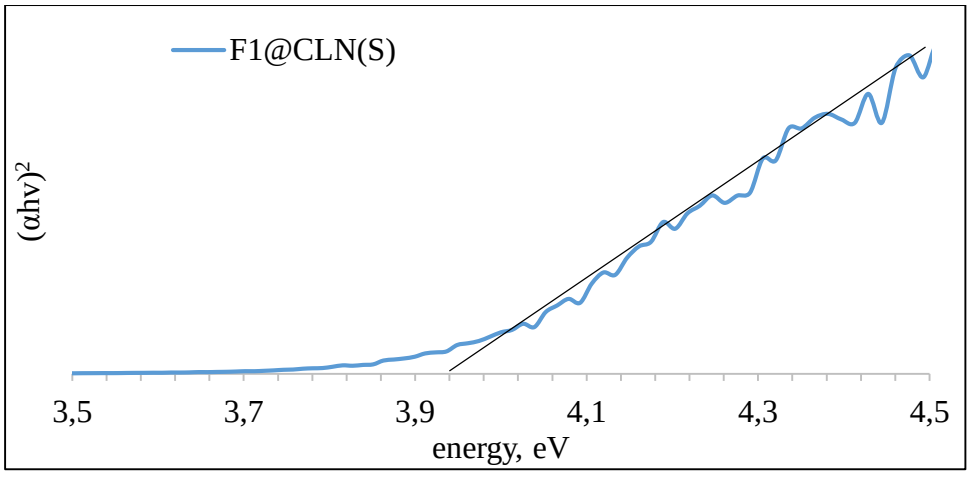

Figure 4. 35. Energy band gap plot of F1@CLN(S)

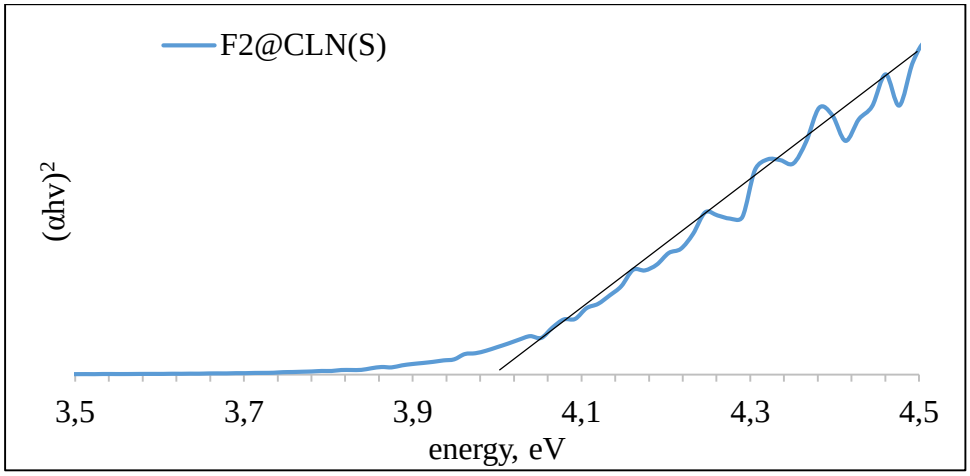

Figure 4. 36. Energy band gap plot of F2@CLN(S)

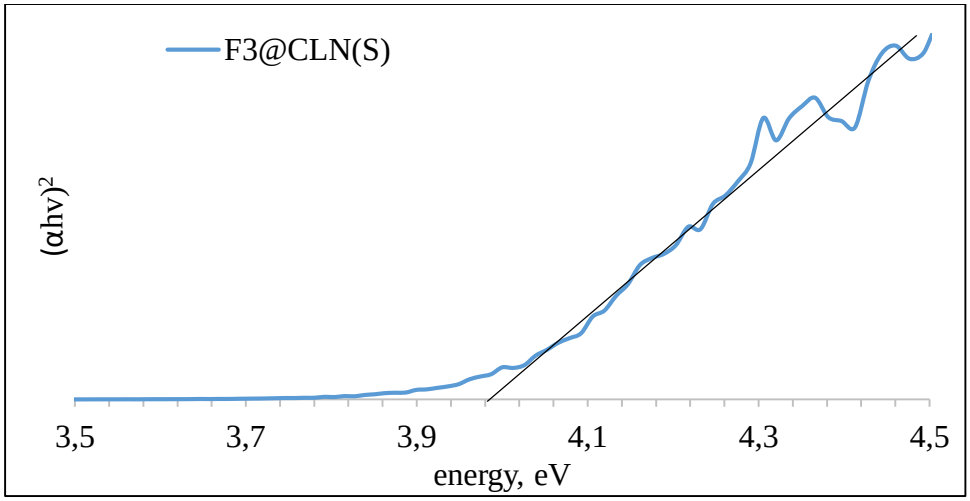

Figure 4. 37. Energy band gap plot of F3@CLN(S)

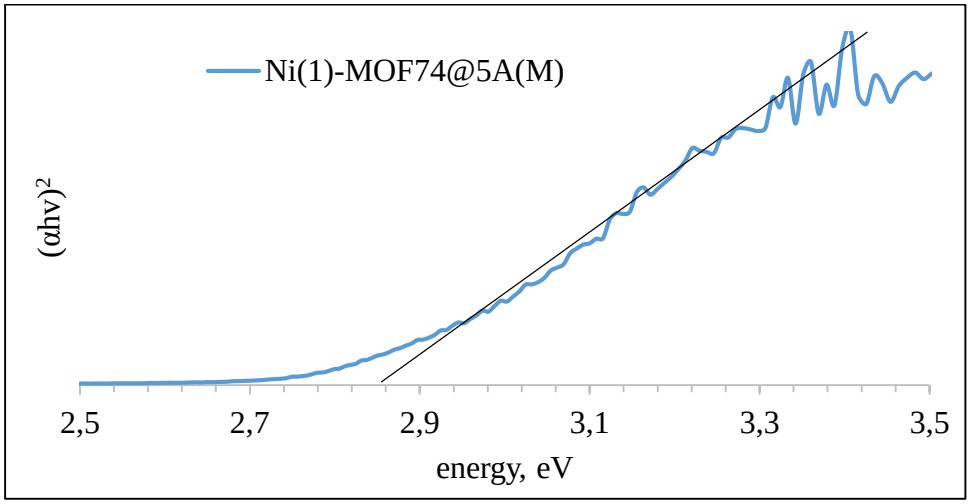

Figure 4. 38. Energy band gap plot of Ni(1)-MOF74@5A(M)

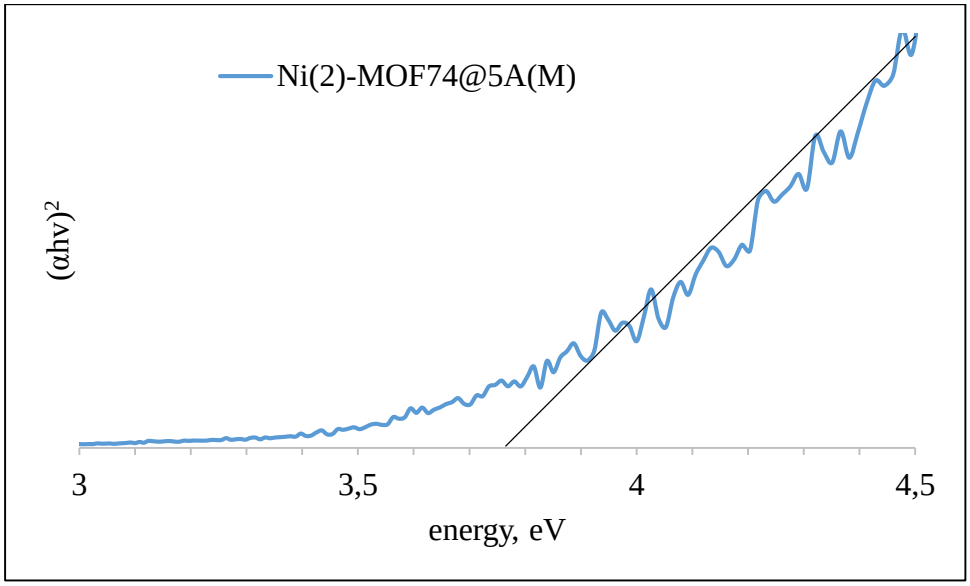

Figure 4. 39. Energy band gap plot of Ni(2)-MOF74@5A(M)

Band gap energy results are given in Table 4.1. Wavelengths which belongs to given band gap energies are tabulated in the table. Wavelengths are changing for each compound. UV band are present between 100-400 nm. Synthesized photocatalysts can be used under UV light except for Ni(1)-MOF-74@5A(M). Its wavelenght is bigger than 400 nm and in this wavelenght visible light is used as light source.

Table 4. 1. Band gap energy results of this study

Compound	**Band Gap Energy, eV**	**Wavelength, nm**
F1	3.76	329
F2	4.05	306
F3	4.04	307
F1@CLN	3.95	314
F2@CLN	4.0	310
F3@CLN	3.94	314
F1@CLN(S)	3.95	313
F2@CLN(S)	4.0	310
F3@CLN(S)	3.98	311
Ni(1)-MOF74@5A(M)	2.86	433
Ni(2)-MOF74@5A(M)	3.78	328

Photocatalytic experiments were done under UV light source. Rhodamine-B degredation were observed by using synthesized photocatalysts. Firstly, adsorption was observed. At time 0 light source was opened. Then, effect of UV light on Rhodamine-B degredation was observed. It can be seen at Figure 4.40 and Figure 4.41 increasing photocatalyst amount is accelerated dye degredation. Additionally, ZIF8(2)@CLN is a better catalyst than F1@CLN(S) by comparing in the experiment with the same amount of photocatalyst.

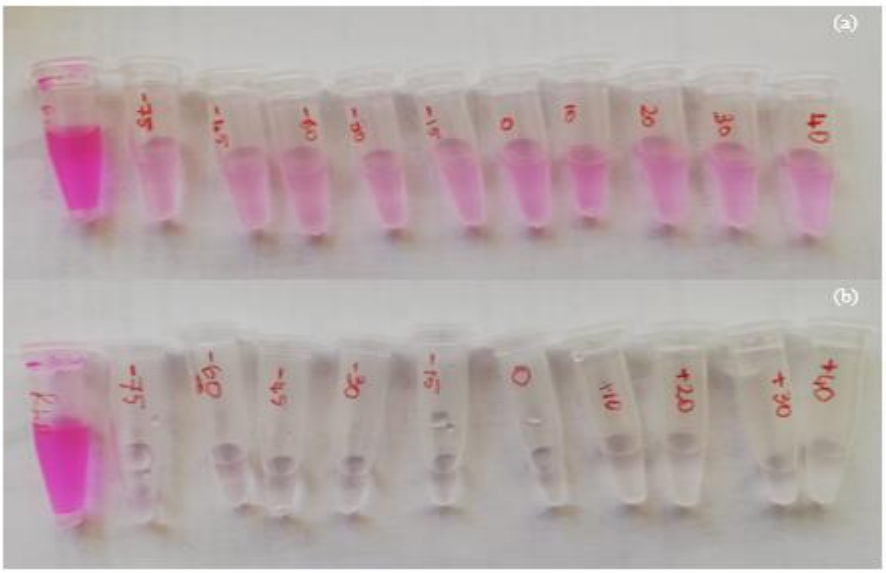

Figure 4. 40. Photocatalytic experiment results of 50 ml RhodB+50 mg ZIF8(2)@CLN (a) and 50 mg RhodB+100 mg ZIF8(2)@CLN (b)

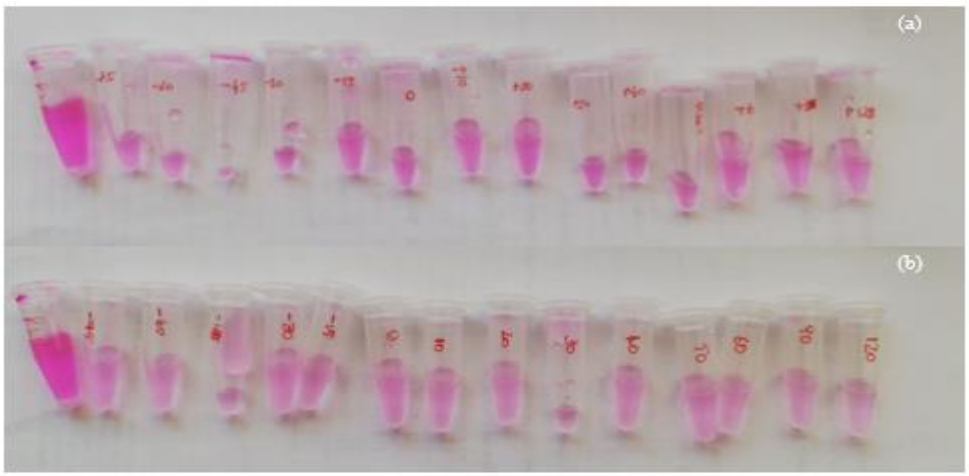

Figure 4. 41. Photocatalytic experiment results of 50 ml RhodB+50 mg F1@CLN(S) (a) and 50 mg RhodB+100 mg F1@CLN(S) (b)

Table 4. 2. Summary of this study

Name of support	**13X**	**Clinoptilolite**	**Alpha alumina**	**5A**
Pretreatment	Aptes modification	Aptes modification Seeding	Aptes modification	Aptes modification
Name of composite	13X(M)	CLN(M) CLN(S)	α(M)	5A(M) Ni(1)-MOF74@5A(M) Ni(2)-MOF74@5A(M)
Metal source	-	Zinc oxide Copper nitrate haxahydrate Zinc nitrate hexahydrate	-	Nickel (II) nitrate hexahydrate
Organic ligand	-	2-methyl imidazole Trimesic acid	-	2,5-dihydroxyterephtalic acid
Process	-	Solvothermal method	-	Solvothermal method
Temperature	-	Room temperature	-	100 °C
Time	-	1 min 10 hour	-	24 h

Summary of this study is given in Table 4.2.

CHAPTER 5

CONCLUSION

Nickel and zinc based organic frameworks and their composites with zeolites were investigated. Surface modification and seeding methods were used to treat the surface of zeolites by seeding or modifying. These treatments help to synthesize MOF on the zeolite.

Characterization studies was performed to understand MOFs and their composites were synthesized successfully or not. These studies were done with XRD, ATR-IR and SEM to all the synthesized samples. Crystalline structure, framework vibration and surface morphology were analyzed. According to these analysis surface modification did not affect to the surface of support. In spite of that a layer was created onto the surface of zeolite with sedding method. Additionally, MOFs were synthesized successfully. Then these MOFs were coated onto the surface of zeolites. Nickel based MOF was coated onto the modified 5A surfaces. ZIF8(2) was coated onto the natural zeolites surface. Also ZIF8/CuBTC composite was synthesized successfully and seeding onto the clinoptilolite surface was performed. Additionally, ZIF8/CuBTC composite was coated onto the surface of clinoptilolite.

Band gap energies of these materials were calculated. Energies were between the 300-450 nm. 100-400 nm refers to the UV range. Photocatalysts which synthesized in this study were used under UV light. Barely, Ni(1)-MOF74@5A(M) sample was used in visible light since the band gap energy. In addition to this, UV light experiments showed that dye degradation was increased with increasing photocatalyst amount.

REFERENCES

Al-Naddaf, Q., H. Thakkar, and F. Rezaei. 2018. "Novel Zeolite-5A@MOF-74 Composite Adsorbents with Core-Shell Structure for H2 Purification." *ACS Appl Mater Interfaces* 10 (35):29656-29666. doi: 10.1021/acsami.8b10494.

Chen, Yongwei, Daofei Lv, Junliang Wu, Jing Xiao, Hongxia Xi, Qibin Xia, and Zhong Li. 2017. "A new MOF-505@GO composite with high selectivity for CO 2 /CH 4 and CO 2 /N 2 separation." *Chemical Engineering Journal* 308:1065-1072. doi: 10.1016/j.cej.2016.09.138.

Christidis, G. 2003. "Chemical and thermal modification of natural HEU-type zeolitic materials from Armenia, Georgia and Greece." *Applied Clay Science* 24 (1-2):79-91. doi: 10.1016/s0169-1317(03)00150-9.

Fujie, K., Otsubo, K., Ikeda, R., Yamada, T., & Kitagawa, H. 2015. "Low temperature ionic conductor: ionic liquid incorporated within a metal–organic framework." *Chemical science 6*(7), 4306-4310. doi: 10.1039/c5sc01398d

Grant Glover, T., Gregory W. Peterson, Bryan J. Schindler, David Britt, and Omar Yaghi. 2011. "MOF-74 building unit has a direct impact on toxic gas adsorption." *Chemical Engineering Science* 66 (2):163-170. doi: 10.1016/j.ces.2010.10.002.

Gupta, V. K., P. J. M. Carrott, M. M. L. Ribeiro Carrott, and Suhas. 2009. "Low-Cost Adsorbents: Growing Approach to Wastewater Treatment—a Review." *Critical Reviews in Environmental Science and Technology* 39 (10):783-842. doi: 10.1080/10643380801977610.

Jafari, Saeed, Farshid Ghorbani-Shahna, Abdulrahman Bahrami, and Hossein Kazemian. 2018. "Adsorptive removal of toluene and carbon tetrachloride from gas phase using Zeolitic Imidazolate Framework-8: Effects of synthesis method, particle size, and pretreatment of the adsorbent." *Microporous and Mesoporous Materials* 268:58-68. doi: 10.1016/j.micromeso.2018.04.013.

Lee, Yu-Ri, Min-Seok Jang, Hye-Young Cho, Hee-Jin Kwon, Sangho Kim, and Wha-Seung Ahn. 2015. "ZIF-8: A comparison of synthesis methods." *Chemical Engineering Journal* 271:276-280. doi: 10.1016/j.cej.2015.02.094.

Li, H., X. Feng, D. Ma, M. Zhang, Y. Zhang, Y. Liu, J. Zhang, and B. Wang. 2018. "Stable Aluminum Metal-Organic Frameworks (Al-MOFs) for Balanced CO2 and Water Selectivity." *ACS Appl Mater Interfaces* 10 (4):3160-3163. doi: 10.1021/acsami.7b17026.

Li, Hao, Zhedong Lin, Xin Zhou, Xiujun Wang, Yingwei Li, Haihui Wang, and Zhong Li. 2017. "Ultrafast room temperature synthesis of novel composites Imi@Cu-BTC with improved stability against moisture." *Chemical Engineering Journal* 307:537-543. doi: 10.1016/j.cej.2016.08.128.

Liu, Yang, Zhifeng Liu, Danlian Huang, Min Cheng, Guangming Zeng, Cui Lai, Chen Zhang, Chengyun Zhou, Wenjun Wang, Danni Jiang, Han Wang, and Binbin Shao. 2019. "Metal or metal-containing nanoparticle@MOF nanocomposites as a promising type of photocatalyst." *Coordination Chemistry Reviews* 388:63-78. doi: 10.1016/j.ccr.2019.02.031.

Ma, Yunan, Chunjie Yan, Aref Alshameri, Xiumei Qiu, Chunyu Zhou, and Dan li. 2014. "Synthesis and characterization of 13X zeolite from low-grade natural kaolin." *Advanced Powder Technology* 25 (2):495-499. doi: 10.1016/j.apt.2013.08.002.

Mohaghegh, Neda, Masoud Faraji, and Amir Abedini. 2018. "Highly efficient multifunctional Ag/TiO2 nanotubes/Ti plate coated with MIL-88B(Fe) as a photocatalyst, adsorbent, and disinfectant in water treatment." *Applied Physics A* 125 (1). doi: 10.1007/s00339-018-2324-8.

Tate, Kirby L., Shiguang Li, Miao Yu, and Moises A. Carreon. 2016. "Zeolite adsorbent-MOF layered nanovalves for CH4 storage." *Adsorption* 23 (1):19-24. doi: 10.1007/s10450-016-9813-x.

Wu, Xiaofei, Zongbi Bao, Bin Yuan, Jun Wang, Yingqiang Sun, Hongmei Luo, and Shuguang Deng. 2013. "Microwave synthesis and characterization of MOF-74

(M=Ni, Mg) for gas separation." *Microporous and Mesoporous Materials* 180:114-122. doi: 10.1016/j.micromeso.2013.06.023.

Xu, Qin, Yanjuan Wang, Gendi Jin, Dangqin Jin, Kexin Li, Airong Mao, and Xiaoya Hu. 2014. "Photooxidation assisted sensitive detection of trace Mn2+ in tea by NH2-MIL-125 (Ti) modified carbon paste electrode." *Sensors and Actuators B: Chemical* 201:274-280. doi: 10.1016/j.snb.2014.05.017.

Yang, S. J., J. H. Im, T. Kim, K. Lee, and C. R. Park. 2011. "MOF-derived ZnO and ZnO@C composites with high photocatalytic activity and adsorption capacity." *J Hazard Mater* 186 (1):376-82. doi: 10.1016/j.jhazmat.2010.11.019.

Yang, C., Miao, G., Pi, Y., Xia, Q., Wu, J., Li, Z., & Xiao, J. 2019. "Abatement of various types of VOCs by adsorption/catalytic oxidation: A review." *Chemical Engineering Journal* 1128-1153. doi:10.1016/j.cej.2019.03.232

Yue, Yanfeng, Bingkun Guo, Zhen-An Qiao, Pasquale F. Fulvio, Jihua Chen, Andrew J. Binder, Chengcheng Tian, and Sheng Dai. 2014. "Multi-wall carbon nanotube@zeolite imidazolate framework composite from a nanoscale zinc oxide precursor." *Microporous and Mesoporous Materials* 198:139-143. doi: 10.1016/j.micromeso.2014.07.026.

Zhang, Q., B. Li, and L. Chen. 2013. "First-principles study of microporous magnets M-MOF-74 (M = Ni, Co, Fe, Mn): the role of metal centers." *Inorg Chem* 52 (16):9356-62. doi: 10.1021/ic400927m.

Zhu, Guanghui, Richard Graver, Laleh Emdadi, Baoyu Liu, Kyu Yong Choi, and Dongxia Liu. 2014. "Synthesis of zeolite@metal–organic framework core–shell particles as bifunctional catalysts." *RSC Advances* 4 (58). doi: 10.1039/c4ra03129f.